Published in final edited form as:
Neuron. 2007 July 5; 55(1): 53–68. doi:10.1016/j.neuron.2007.05.030.

Polarized signaling endosomes coordinate BDNF-induced chemotaxis of cerebellar precursors

Pengcheng Zhou[2,1], **Marimelia Porcionatto**[2,1,3], **Mariecel Pilapil**[2], **Yicheng Chen**[2], **Yoojin Choi**[2], **Kimberley F. Tolias**[4,5], **Jay B. Bikoff**[4], **Elizabeth J. Hong**[4], **Michael E. Greenberg**[4], and **Rosalind A. Segal**[2,6]

2 *Department of Pediatric Oncology, Dana-Farber Cancer Institute and Department of Neurobiology, Harvard Medical School*

4 *Division of Neuroscience, Children's Hospital Boston and Department of Neurobiology, Harvard Medical School*

Summary

During development, neural precursors migrate in response to positional cues such as growth factor gradients. However, the mechanisms that enable precursors to sense and respond to such gradients are poorly understood. Here we show that cerebellar granule cell precursors (GCPs) migrate along a gradient of brain-derived neurotrophic factor (BDNF), and we demonstrate that vesicle trafficking is critical for this chemotactic process. Activation of TrkB, the BDNF receptor, stimulates GCPs to secrete BDNF, thereby amplifying the ambient gradient. The BDNF gradient stimulates endocytosis of TrkB and associated signaling molecules, causing asymmetric accumulation of signaling endosomes at the subcellular location where BDNF concentration is maximal. Thus regulated BDNF exocytosis and TrkB endocytosis enable precursors to polarize and migrate in a directed fashion along a shallow BDNF gradient.

Introduction

Chemotaxis is an oriented cell migration wherein a cell becomes polarized with a defined front and back, enabling the cell to move in a forward direction toward an attractive agent (Ridley et al., 2003; Vicente-Manzanares et al., 2005; Webb et al., 2005). Genetic and mechanistic studies have identified many of the molecules required for the complex interactions among substrate, membrane and cytoskeleton that allow movement (Affolter and Weijer, 2005; Dujardin et al., 2003; Fishell and Hatten, 1991; Myers et al., 2005; Nagano et al., 2004; Nagano et al., 2002; Qin et al., 2000; Snapper et al., 2005). However, the mechanisms that lead to polarization and directional migration in response to extracellular cues are not well understood.

Chemotaxis is critical for neural development, as neural precursors travel long distances from proliferative zones to reach the correct positions for mature function. At particular stages in development, precursors travel in predictable directions and along defined axes. While early

[6] To whom correspondence should be addressed: Rosalind A. Segal, Department of Pediatric Oncology, Dana-Farber Cancer Institute, 44 Binney Street, Boston, MA 02115, 617-632-4737, 617-632-2085, Rosalind_segal@dfci.harvard.edu.
[1]The first two authors contributed equally.
[3]Current address: Department of Biochemistry, Federal University of São Paulo, São Paolo, Brazil.
[5]Current address: Department of Neuroscience, Baylor College of Medicine

precursors migrate tangentially along a rostral-caudal or circumferential path, both cerebral and cerebellar precursors migrate radially at defined developmental stages. Neurons of the cerebral cortex travel outward from the ventricular zone to the cortical layers, while cerebellar granule cell precursors (GCPs) travel radially inward from a proliferative zone in the external granule cell layer (EGL) and traverse the molecular layer to reach the internal granule cell layer (IGL) (Hatten, 1999, 2002; Komuro and Yacubova, 2003; Komuro et al., 2001; Nadarajah et al., 2002). During radial migration, precursors often migrate along glial "tracks" that restrict migration decisions to a simple choice: the cells can remain stationary, they can move forward or move backward (Nadarajah et al., 2001; Rakic, 1971; Rivas and Hatten, 1995). Precursors move relatively slowly during radial migration, at rates of approximately 10–30 μm/hour, and so migration of GCPs from the EGL to the IGL occurs over the course of several days *in vivo* (Bellion et al., 2005; Edmondson and Hatten, 1987; Fishell and Hatten, 1991; Komuro et al., 2001; Nadarajah and Parnavelas, 2002). Once GCPs reach the appropriate location in the IGL, migration ceases. Together these attributes make it possible to examine the mechanisms that regulate radial migration of GCPs *in vitro, in vivo* or in organotypic slice cultures.

The cytoskeletal changes required for radial migration include remodeling of the microtubule network that surrounds the nucleus and extends forward to a centrosome positioned in front of the nucleus. In addition, changes of the actin cytoskeleton and associated myosin motors enable the leading process to move forward and the trailing process to retract as the cell migrates. These cytoskeletal changes are regulated by intracellular molecular components that orchestrate cell polarity (Bielas and Gleeson, 2004; Hatten, 2002; Tsai and Gleeson, 2005).

In order for cells to move in the appropriate direction *in vivo*, extracellular cues must regulate these polarity molecules. Among the possible attractive cues are neurotrophins (Borghesani et al., 2002; Jones et al., 1994; Polleux et al., 2002; Yamauchi et al., 2003; Yoshizawa et al., 2005), chemokines (Klein et al., 2001; Zhu et al., 2002), netrins (Bloch-Gallego et al., 1999; Hamasaki et al., 2001; Yee et al., 1999), semaphorins (Bagnard et al., 2001; Gammill et al., 2006; Kerjan et al., 2005) and ephrins (Conover et al., 2000; Lu et al., 2001; Santiago and Erickson, 2002), while repulsive cues include slit (Brose and Tessier-Lavigne, 2000; Kramer et al., 2001; Piper and Little, 2003; Wu et al., 1999), and netrin (Hamasaki et al., 2001). Brain-derived neurotrophic factor (BDNF) is an extracellular factor that regulates neural precursor migration. *In vivo*, neural migration is abnormal in the cerebral and cerebellar cortex of mutant mice that lack or overexpress BDNF, and BDNF can stimulate migration of precursors in tissue culture system (Borghesani et al., 2002; Jones et al., 1994; Polleux et al., 2002; Ringstedt et al., 1998). However, it is not yet known whether this ligand is involved in movement per se, and/or in the directionality of the response. Here we show that a gradient of BDNF exists in the developing cerebellum, and GCPs migrate along the BDNF gradient that can both orient and stimulate migration. Correct orientation of migration depends on TrkB-dependent secretion of BDNF by GCPs and subsequent accumulation of activated TrkB receptors in endosomes located in or adjacent to the leading process. We identify Tiam1/Rac and PI (3, 4, 5) P3 (PIP3) phospholipids as critical components in the chemotactic response to BDNF and demonstrate that these components colocalize with TrkB in signaling endosomes at the leading process. Thus, TrkB-regulated BDNF release and localized endocytosis of BDNF/TrkB constitute mechanisms that enable GCPs to establish an intracellular gradient of signaling components steeper than the shallow extracellular BDNF gradient, so that GCPs migrate directionally.

Results

BDNF promotes directed radial migration of granule cell precursors

In *bdnf* −/− mice, migration of GCPs from the EGL to IGL is impaired (Borghesani et al., 2002). An extracellular factor such as BDNF might stimulate migration with or without

providing a directional cue. As an *in vivo* gradient is needed for a factor to provide a directional cue, we investigated the distribution of BDNF protein in the developing cerebellum. We examined BDNF concentrations in lysates of EGL and IGL microdissected at postnatal day 7 (P7), a stage when the GCPs are actively migrating. As shown in Supplemental Figure 1A, the BDNF concentration as determined by ELISA is two-fold higher in IGL than in EGL. Taken together with previous studies of BDNF expression by *in situ* hybridization and immunostaining (Borghesani et al., 2002; Rocamora et al., 1993; Wetmore et al., 1990), these results indicate that regulated expression of BDNF *in vivo* generates a gradient that increases along the migratory path from the EGL to the IGL.

To investigate the role of BDNF as a chemotactic factor for neural precursors, we established an *in vitro* real-time migration assay (Supplemental Figure 1B), wherein GCPs purified from P6 mice are exposed to an exogenous BDNF gradient and observed by time-lapse microscopy. As shown in Supplemental Figure 1B, BDNF loaded into the agarose plug diffuses into the medium, creating a sharp gradient of BDNF as validated by ELISA (Supplemental Figure 1C). Using this experimental system, we traced the migratory paths of individual GCPs during two hours of data acquisition under control condition, when exposed to a BDNF gradient, or when exposed to a uniform distribution of BDNF. For each condition, we superimposed the paths of each GCP from four experiments on a common origin to generate the composites shown in Figure 1A. As shown, while both uniform BDNF and a BDNF gradient increased the percentage of cells that migrate compared to control condition, the gradient had a greater effect (Figure 1B). Furthermore, we find that cells migrate in a random direction in control or uniform BDNF condition, but preferentially migrate toward the BDNF source in the gradient condition (Figure 1C and Supplemental movie). Thus, BDNF promotes migration most effectively when presented as a gradient, and it provides a directional cue for movement.

Mathematical modeling of chemotactic responses has indicated that basal migration can be modeled by a random walk; chemotactic responses can often be modeled as a biased random walk with high coefficient of non-randomness (μ) (Shreiber et al., 2003). As shown in Figure 1D, the BDNF gradient significantly increased μ compared with control or uniform BDNF conditions, without significantly altering other attributes of migration, such as velocity (Supplemental Figure 2), or duration (data not shown). Thus BDNF functions as a chemotactic factor, converting the stationary state or random walk of precursors under basal conditions into a directed random walk that is oriented towards the BDNF source.

BDNF activation and redistribution of TrkB mediates directional migration

BDNF has two potential receptors: TrkB and p75NTR, both of which are expressed by GCPs and could be involved in BDNF-induced chemotaxis (Carter et al., 2003; Klein et al., 1990; Segal et al., 1995). To distinguish the receptor pathway(s) required for BDNF induced directed migration of GCPs, we used both pharmacologic and genetic approaches. We find that K252a, an agent that prevents Trk kinase activity (Berg et al., 1992; Tapley et al., 1992), markedly inhibits directed migration of GCPs (Figure 1E). Treatment with K252a not only reduces the percentage of migratory cells, but also reduces the directional movement of GCPs toward the BDNF source (Figure 1F). We find that K252a also prevents GCP migration in an organotypic slice culture (Figure 1G), demonstrating that this Trk inhibitor can prevent migration in response to endogenous neurotrophin. We have validated that K252a, at the dose used, prevents BDNF-induced activation of TrkB (inserted blot of Figure 1E) and its downstream signaling components (data not shown). Because GCPs express p75NTR as well as TrkB, and p75NTR has been implicated in Schwann cell migration during development (Bentley and Lee, 2000), we tested the migration of GCPs prepared from p75NTR exon III mutant mice (Lee et al., 1992). BDNF increased both migration and directed movement of p75 mutant cells as observed for wild type cells (Figure 1H). Taken together with previous *in vivo* analyses of various TrkB

(Medina et al., 2004; Minichiello and Klein, 1996) and p75NTR mutants (Carter et al., 2003), these data demonstrate that TrkB, but not p75NTR, mediates BDNF-induced chemotactic response of GCPs.

A chemotactic response requires polarization of the intracellular cytoskeleton, resulting in elongation of a leading process directed up the gradient. The leading process features prominent actin filaments. As shown in Figure 2A, in response to BDNF stimulation, GCPs extend a leading process toward the source of BDNF; this leading process contains abundant actin filaments that can be visualized with fluorescent phalloidin. We find that TrkB receptors are localized in the leading process (Figure 2A5–A8), and are oriented toward the source of BDNF (Figure 2B). Moreover, TrkB receptors concentrated in the leading process are activated receptors, and can be visualized using an anti-phospho-Trk antibody (anti-pY490) (Figure 2C). These results indicate that TrkB is activated and relocalized in response to a BDNF gradient. Other receptors expressed by the GCPs do not accumulate in the leading process, as shown by immunostaining with antibodies to CXCR4 (data not shown), a chemokine receptor expressed by the GCPs (Klein et al., 2001; Lu et al., 2001; Zhu et al., 2002).

We find that TrkB also relocalizes in response to uniform BDNF stimulation. However, under these conditions, the probability that TrkB will accumulate at the side of the cell facing the agarose plug is equal to the probability that TrkB will accumulate at the opposite side of the cell (in control and uniform conditions the agarose plug is loaded with vehicle) (Figure 2B). This is in striking contrast to the localization of TrkB in response to a gradient, where TrkB is more than twice as likely to accumulate at the side of the cell facing the agarose plug that is the source of BDNF rather than at the opposite side of the cell. These data indicate that polarized localization of TrkB receptors to the site of maximal BDNF concentration may be an important component determining directionality of the chemotactic response.

The migration assay used here enables us to distinguish a directed migratory response from a generalized increase in motility, and so is appropriate for studies of BDNF-induced chemotaxis. However, GCPs extend a relatively short leading process when migrating along a laminin substrate, instead of on a radial glial fiber. To determine whether TrkB is also localized to the more elaborated leading processes of GCPs migrating along glial fibers, we examined TrkB distribution in GCP/Bergmann glia cocultures stimulated with BDNF. As shown, TrkB (red) can be seen at the front of the GCP soma (green) and also in the leading process of this migrating cell (Figure 2D and 2E). Thus, when GCPs are migrating either on a laminin substrate or along a Bergmann glial fiber, TrkB receptors localize to the leading processes of GCPs moving in response to BDNF stimulation. Furthermore, in the presence of a BDNF gradient, TrkB receptors preferentially localize to the cellular site where BDNF is at a maximal concentration.

TrkB receptors in the leading processes of stimulated GCPs have a punctate distribution, and appear to be inside the limits of the plasma membrane. Therefore, we asked whether these puncta represent endosomes. To do so, we used an antibody against α-adaptin, an endocytic component enriched in early endosomes (Gonzalez-Gaitan and Jackle, 1997; Robinson, 1994; Takei and Haucke, 2001). As shown, internalized TrkB receptors colocalize with α-adaptin and other early endosomal markers after BDNF stimulation (Figure 2F and data not shown), indicating that these receptors are located in an endosomal compartment.

To determine whether redistribution of TrkB to endosomes in the leading process also occurs *in vivo*, and so might orchestrate radial migration during development, we examined the localization of TrkB in GCPs as they migrate from the inner portion of the EGL towards the IGL. Our results reveal that TrkB receptors are enriched in punctate structures within a crescent or extended process at the front of GCPs (Figure 3A, A1–A4). The identity of these cells as GCPs was verified by the expression of Zic, a marker of the granule cell lineage (Aruga et al.,

1994) (Figure 3A). To determine whether localization of TrkB receptors to the leading process *in vivo* requires a BDNF gradient, we investigated TrkB localization in *bdnf −/−* mice. In contrast to the polarized localization of TrkB puncta seen in wild type animals, TrkB immunostaining in *bdnf −/−* mice exhibits a random distribution pattern (Figure 3A5–A8; 3C and 3D), similar to that seen in unstimulated GCPs *in vitro* (Figure 2A). While TrkB clusters in GCPs are directed toward the IGL in wild type mice, TrkB clusters in GCPs from *bdnf −/−* mice are more often directed toward or parallel to the pia, and thus point in the wrong direction for radial migration. Consistent with our studies *in vitro*, TrkB receptors located in the leading processes of wild type GCPs *in vivo* are predominantly in endosomes that can be immunostained with antibodies to α-adaptin (Figure 3B, B1–B4) (65% and 54% of TrkB pixels colocalize with α-adaptin in wild type and *bdnf −/ −*mice, respectively. N=5, $p < 0.05$), thus the polarization of TrkB signaling endosomes *in vivo* depends on the presence of a BDNF gradient. Together these data indicate that a chemotactic response to BDNF involves relocalization of activated TrkB receptors to endosomes at the cellular site where BDNF is maximal, and these endosomes mark the direction of movement.

TrkB endocytosis is required for directed cell migration

The data above suggest that trafficking of vesicular TrkB receptors might coordinate directed migration of GCPs. While receptor endocytosis was previously viewed as a mechanism for receptor downregulation and degradation (Burke et al., 2001; Di Fiore and De Camilli, 2001), accumulating evidence indicates that intracellular trafficking of signaling endosomes can be important in executing a ligand-initiated response (Beattie et al., 1996; Heerssen et al., 2004; Howe, 2005; Howe and Mobley, 2004; Jekely et al., 2005). This is particularly true for the Trk receptors, which remain activated for prolonged periods of time following neurotrophin stimulation (Ginty and Segal, 2002). To address the timing and extent of receptor endocytosis in GCPs, we used a biochemical approach in which we analyze surface receptors by biotinylation. We find that the proportion of TrkB located at the cell surface of GCPs declines with increased time of BDNF stimulation (Figure 4A and B). The time course of internalization is fairly slow, and there is a significant lag between internalization and degradation of the receptor (Figure 4B and C).

To determine whether this slow endocytosis of TrkB receptors might be required for directed migration, we used monodansyl cadaverine (MDC), a pharmacologic agent that inhibits internalization of surface membrane molecules (Davies et al., 1980; Heerssen et al., 2004). Treatment of GCPs with MDC prevents BDNF-induced TrkB receptor endocytosis (lower panel, Figure 4E), while there is no effect on TrkB signaling (Figure 4D). We find that MDC significantly reduces the percentage of cells that migrate in response to a BDNF gradient (Figure 4E). Further analysis of the paths taken by motile cells revealed that MDC treatment completely abrogates the directionality of GCP migration (Figure 4F). In contrast, MDC actually increases the percentage of cells that migrate in the absence of BDNF (Figure 4F), indicating that this treatment does not interfere with the mechanics of movement. The inhibitory effect of MDC on directed migration of GCPs was recapitulated in organotypic slice culture (Figure 4G–I), indicating that endocytosis is required for migration of GCPs stimulated by endogenous BDNF. These data suggest that endocytosis of TrkB receptors is required for a chemotactic response to BDNF.

We next used a molecular approach to verify that endocytosis of Trk receptors is needed for GCP migration. We used a dominant-negative form of dynamin (K44A mutant), which interferes with both clathrin-dependent and clathrin-independent endocytosis (Damke et al., 1994; Robinson, 1994; van der Bliek et al., 1993). Previous studies indicate that dynamin function is needed for endocytosis of activated Trk receptors and other membrane proteins (Damke et al., 1994; Grimes et al., 1996; Robinson, 1994; Valdez et al., 2005; van der Bliek

et al., 1993; Zhang et al., 2000). As shown, when we infect organotypic cerebellar slices with a lentivirus expressing dynamin K44A and GFP, most GFP-positive GCPs are unable to migrate out of the EGL, and remain there three days later (Figure 4K). In contrast, when a slice culture is infected with control lentivirus expressing wild type dynamin and GFP, virtually all the GFP-positive GCPs migrate out of the EGL within three days (Figure 4J and L). Thus, expression of dominant-negative dynamin K44A, like treatment with MDC, markedly inhibits migration of GCPs in slice cultures responding to endogenous neurotrophins. Together these findings indicate that endocytosis of TrkB receptors is critical for BDNF-stimulated cell polarization and chemotaxis.

BDNF functions as an autocrine ligand to amplify the local gradient

In previous studies we found that migration of GCPs out of the EGL is impaired in *bdnf −/−* mice *in vivo*, and that GCPs of these animals exhibit decreased migration in tissue culture assays (Borghesani et al., 2002). As shown in Figure 5A, both gradient and uniform BDNF increase migration of *bdnf −/−* GCPs. However, in contrast to results observed with wild type cells, uniform BDNF stimulates migration of mutant GCPs to the same extent as the BDNF gradient. Furthermore, unlike wild type cells, GCPs of *bdnf −/−* mice migrate randomly in response to a BDNF gradient (Figure 5B and 5C). Thus an exogenous BDNF gradient can stimulate migration of mutant cells, but the cells cannot recognize or respond to the gradient in a directionally appropriate manner.

These findings provide us with a system that dissociates BDNF-induced motility from BDNF-induced directionality, and so can be used to determine the mechanisms whereby a cell polarizes correctly with a leading process at the location of maximal BDNF concentration. To ascertain whether polarized accumulation of TrkB in the leading process is needed to orient migration up the BDNF gradient, we visualized TrkB-containing signaling endosomes in GCPs of *bdnf −/−* mice. As shown in Figure 5D and E, TrkB does redistribute to endosomes that accumulate at one side of the mutant cells in response to a BDNF gradient. However, in *bdnf −/−* GCPs, the location where signaling endosomes accumulate is random relative to the BDNF gradient (Figure 5D). These studies suggest that *bdnf −/−* GCPs migrate randomly *in vitro* because signaling endosomes are not correctly polarized. Taken together, we conclude that a BDNF gradient induces polarized accumulation of signaling endosomes in leading processes of wild type GCPs both *in vivo* and *in vitro*, and that the location of the signaling endosomes dictates the direction of migration.

The specific deficit in chemotaxis of *bdnf −/−* cells could reflect a cell autonomous requirement for BDNF in order to initiate directed migration. Alternatively, precursors obtained from *bdnf −/−* mice might acquire additional deficits that preclude a chemotactic response. To distinguish these possibilities, we asked whether acute reduction in BDNF recapitulates the mutant phenotype. Using lentivirus to express siRNA for BDNF, we successfully reduced by 80% the level of BDNF protein in GCPs (Figure 6A). As shown in Figures 6B and C, GCPs expressing *bdnf* RNAi exhibited impaired chemotaxis in response to a BDNF gradient. In contrast, GCPs treated in parallel with a control virus remained capable of directed chemotaxis. The data with acute BDNF knock-down are similar to the results obtained using GCPs from *bdnf −/−* mice (Compare figures 6B and 5A, and figure 6CD and 5C). Thus, BDNF expression and secretion by GCPs are required for a chemotactic response to an exogenous ligand gradient.

These findings suggest the intriguing possibility that autocrine BDNF might amplify the BDNF gradient and so enhance the directed migration. Previous studies have shown that neurotrophins themselves can induce neurotrophin secretion in transfected PC12 cells (Canossa et al., 1997; Kruttgen et al., 1998), in astrocytes (Lambert et al., 2004) and in neurons (Canossa et al., 1997). We therefore asked whether exposing GCPs to a BDNF gradient might induce BDNF release and thereby amplify the local gradient. To address this question, we stimulated GCPs

with Neurotrophin 4 (NT4). While NT4 is able to stimulate TrkB activation, endocytosis and signaling (Minichiello et al., 1998; Yuen and Mobley, 1999), the ligand is antigenically distinct from BDNF, and so we can monitor release of endogenous BDNF in response to NT4. As shown in Figure 6E, stimulation of GCPs with NT4 causes BDNF secretion. Based on the timing and the amount of BDNF released per cell (approximately 1.2 x 10^{-7} femptomole/cell released within 6 hours), stimulated secretion of BDNF could amplify the local concentration gradient and so facilitate a chemotactic response.

Given that BDNF is released by GCPs in response to TrkB activation, we asked whether BDNF functions in an autocrine manner to stimulate directed migration of GCPs. To do so we analyzed migration of GCPs in organotypic slice cultures following infection with lentivirus expressing *bdnf* siRNA together with GFP. We monitor migration by pulse labeling GCPs with BrdU, then allowing 36 hours for BrdU-positive cells to migrate from the EGL to the IGL. As shown in Figure 6F and G, the GFP-positive GCPs expressing *bdnf* siRNA exhibit reduced migration compared with GCPs infected with a control virus. However, migration of the surrounding non-infected GCPs is not affected by the *bdnf* siRNA construct. Thus, BDNF is required in a cell autonomous fashion for GCP chemotaxis in the slice cultures. Together these data suggest a model wherein the perceived intracellular gradient is amplified in two ways: first by BDNF-stimulated BDNF release, and second by localized accumulation of BDNF/TrkB-containing signaling endosomes at the site where BDNF concentration is maximal.

PI3 kinase and Tiam1/Rac mediate BDNF-induced chemotaxis

To determine the mechanism by which localized, endocytosed TrkB receptors orchestrate directed migration of GCPs, we asked which of the many signaling pathways activated by TrkB are required for directed migration (Huang and Reichardt, 2003). In non-neural systems both the phosphatidylinositol kinase (PI3K) and mitogen-activated protein kinase (MAPK) pathways have been implicated in chemotaxis, and these pathways are activated by TrkB signaling (Funamoto et al., 2002; Huang et al., 2004). Pharmacologic reagents allow us to inhibit the endogenous signaling molecules beginning at the time that we initiate the assay, and so enable us to identify pathways directly involved in BDNF-induced migration. Pretreatment of cerebellar GCPs with LY294002, a PI3K inhibitor, completely blocks BDNF-induced GCP migration (Figure 7A) and the directional bias induced by a BDNF gradient (Figure 7B). We verify that this brief treatment selectively interferes with PI3K signaling in GCPs (Figure 7C) but does not interfere with basal migration or affect survival (data not shown). Thus, the PI3K pathway has a critical role both in the increased motility and directional response induced by a BDNF gradient.

In contrast, pretreatment of GCPs with U0126, an inhibitor of the extracellular signal-regulated kinase (Erk) pathway, does not alter BDNF-induced initiation or directionality of migration, even though U0126 treatment clearly interferes with Erk1/2 activation (Supplemental Figure 3). While previous studies indicated that both PI3K and MAPK can contribute to chemotaxis in response to nerve growth factor (NGF) or other extracellular factors (Huang et al., 2004; Iijima et al., 2002; Merlot and Firtel, 2003; Qi et al., 2001; Sawada et al., 2000), only the PI3 kinase pathway is essential for BDNF-induced migration of GCPs.

The products of PI3 kinase, PIP3 phospholipids, can serve as intermediaries that both localize and stimulate activation of Rho-family G-proteins, and might thereby promote cell motility (Affolter and Weijer, 2005; Bokoch et al., 1996; Hawkins et al., 1995; Raftopoulou and Hall, 2004; Sander et al., 1998; Servant et al., 2000). To determine whether PI3 kinase promotes BDNF-induced GCP migration by stimulating Rho family G-proteins, we asked whether this group of proteins is involved in BDNF-induced chemotaxis. Toxin B, which acts quickly to inhibit diverse Rho family GTPases, prevents BDNF-induced migration (Figure 8A). We next asked which family members are activated by BDNF in cerebellar GCPs. We find that BDNF

induces activation of endogenous Rac and cdc42 in GCPs (Figure 8B–D), and that activation of Rac can be abrogated by Toxin B (Figure 8E). We did not detect activation of Rho in response to BDNF (data not shown). These data suggest that BDNF-induced activation of Rac and / or cdc42 is critical for GCP chemotaxis.

During chemotaxis, PIP3 and Rac often activate one another and thereby amplify a subcellular gradient. Surprisingly, in GCPs Rac activation in response to BDNF does not depend on PIP3 phospholipids. As shown, inhibition of BDNF-induced activation of PI3 kinase using LY294002 has no effect on Rac activation (Figure 8F). Activated Rac itself can stimulate PI3 kinase activity under some circumstances (Keely et al., 1997; Tolias et al., 1995; Zheng et al., 1994); however, inhibition of BDNF-induced Rac/cdc42 by toxin B does not prevent PI3 kinase activation (Figure 8G). Thus, BDNF-induced migration requires two independent pathways activated simultaneously, one involving Rac/cdc42 and one involving PI3 kinase. Although these pathways are not dependent on one another, both are indeed downstream of TrkB, as pretreatment of GCPs with K252a abolishes BDNF-induced activation of Rac (Figure 8H) and of PI3 kinase activity (Figure 7C). Taken together, these results demonstrate that activation and internalization of TrkB receptors, as well as PI3 kinase and Rac activation are all essential for BDNF-induced directed migration.

Since Rac activation is not initiated by PIP3 phospholipids in this system, we asked how TrkB stimulates Rac activity. In the developing cerebellum, a Rac-specific guanine nucleotide exchange factor (GEF), Tiam1, is highly expressed in GCPs (Ehler et al., 1997). While Tiam1 is often activated by lipid products of PI3 kinase (Mertens et al., 2003; Miyamoto et al., 2006; Sander et al., 1998), Tiam1 can also be recruited to a signaling complex in a PI3 kinase-independent manner (Lambert et al., 2002). Consistent with recent studies (Miyamoto et al., 2006), we find that in GCPs, endogenous TrkB co-precipitates with endogenous Tiam1 in a BDNF-stimulated manner (Figure 9A), suggesting that this might be a pathway for activation of Rac by internalized TrkB receptors.

To determine whether this pathway is required for directed migration, we used a lentivirus siRNA to reduce expression of Tiam1 (Figure 9B). We find that Tiam1 siRNA, but not control lentivirus, inhibits BDNF-induced Rac activation (Fig. 9B and C). The lentivirus expressing Tiam1 siRNA also blocks BDNF-induced directional migration of GCPs in our real-time migration assay (Figure 9D) and in organotypic slice cultures (Figure 9E–G). Collectively, these results indicate that BDNF activation of TrkB stimulates two parallel pathways, Tiam1/Rac and PI3 kinase, and that both pathways are needed for chemotaxis. We asked whether Tiam1 and phospholipids colocalize with TrkB-containing signaling endosomes. Following BDNF gradient stimulation, the PIP3 phospholipid products of PI3 kinase pathway (Figure 10A) and Tiam1 (Figure 10B) both colocalize with TrkB in endosomes in the leading process, suggesting that these two pathways are spatially coordinated.

Large signaling complexes containing TrkB and downstream signaling molecules also form *in vivo*. As shown, Tiam1 colocalizes with TrkB in GCPs of wild type mice (Figure 10C), and this complex is seen in the leading processes of the cells located at the innermost portion of the EGL. TrkB significantly colocalizes with Tiam1 in wild type mice (67% of TrkB pixels colocalized with Tiam1 in wild type mice while 50% of TrkB pixels colocalized with Tiam1 in *bdnf* −/− mice, n=6, $p < 0.001$), indicating that signaling endosomes containing both TrkB and Tiam1 are selectively localized to the side of the cell with a maximal concentration of BDNF. Thus, both *in vitro* and *in vivo*, TrkB and associated signaling molecules localize to endosomes located at the cellular site facing the BDNF source with maximal concentration. Collectively, these data indicate that endocytosis and localization of complex signaling endosomes to the front of neural precursors are critical elements of the neurotrophin-induced chemotactic response.

Discussion

During development, neural precursors of the cerebral and cerebellar cortex migrate radially from a proliferative zone, traverse the developing cortex, and then cease migrating once they reach their final destination (Hatten, 1999, 2002; Nadarajah and Parnavelas, 2002). Cues that simultaneously increase migration and provide directionality are optimal for regulating this behavior. We find that this is exactly the effect of BDNF. Our results demonstrate that a BDNF gradient not only stimulates motility, but also determines the direction of migration. While a number of other soluble factors and cell-cell interactions undoubtedly contribute to the regulation of GCP migration and so limit the severity of the migration defect in *bdnf* −/− mice (Kerjan et al., 2005; Klein et al., 2001; Komuro and Rakic, 1993; Lu et al., 2001; Rio et al., 1997; Tomoda et al., 2004; Zhu et al., 2002), our data indicate that BDNF functions as a chemotactic factor both *in vivo* and *in vitro*.

A major question in chemotaxis is how cells perceive a subtle gradient and become correctly polarized. We calculate that the difference in BDNF concentration between the front and the back of the granule cell soma is approximately 6% of the BDNF concentration *in vivo*, approximately 0.1 to 0.3 femptomolar in both our *in vivo* and *in vitro* systems. We have identified two mechanisms whereby GCPs amplify the perceived gradient. One simple mechanism for amplifying a gradient is to augment the local concentration of ligand. Consistent with previous studies in other cell types (Saarelainen et al., 2001; Yang et al., 2006), we find that activation of TrkB receptors stimulates release of BDNF from wild type GCPs. This regulated release of ligand cannot occur in GCPs that lack BDNF due to germline mutations or due to acute expression of *bdnf* siRNA. As a result, GCPs that lack BDNF are unable to chemotax properly in response to a BDNF gradient. The timing and extent of BDNF release in response to TrkB activation suggest that regulated release could play an important role in the ability of GCPs to exhibit a chemotactic response to BDNF. If the BDNF released by each cell, approximately 1.2×10^{-7} femptomole, spreads through a volume of 5 microliters, the steepness of the gradient would increase by 8%. This increase would have a significant effect on the gradient itself and hence on migration. The protein CAPS2, which promotes localized and regulated release of BDNF (Sadakata et al., 2004), is likely to be a critical component of this autocrine release of ligand. Indeed, a recent study demonstrated that mice lacking CAPS2 exhibit impaired GCP migration (Sadakata et al., 2007).

A second mechanism that amplifies the gradient is the localized accumulation of TrkB-containing signaling endosomes at the side of the cell where BDNF concentration is maximal. An accumulation of signaling endosomes containing activated TrkB receptors marks the leading processes of wild type GCPs within the inner EGL that are poised to begin migrating. This localized accumulation is not observed in mice that lack BDNF. To determine whether localized accumulation of TrkB-containing signaling endosomes is required for directed migration we used both a dissociated cell migration assay and organotypic slice cultures. Pharmacologic interventions that prevent endocytosis of TrkB receptors inhibit BDNF-induced chemotaxis in a dissociated culture system. In contrast, these pharmacologic interventions do not inhibit basal migration of GCPs, indicating that endocytosis is required for the chemotactic response to BDNF rather than for the mechanics of motility. Similarly, both pharmacologic and genetic inhibitors of Trk endocytosis interrupt migration of GCPs in a slice culture wherein GCPs respond to endogenous chemotactic cues. These findings reveal a crucial role of TrkB receptor endocytosis in the chemotactic response to BDNF.

Although endocytosis has long been regarded as a mechanism of receptor signal attenuation, it is becoming appreciated that the function of endocytosis is not limited to signal downregulation and receptor removal (Le Roy and Wrana, 2005). In neuronal cells receptor endocytosis is involved in long distance signaling (Ginty and Segal, 2002), and is needed to

redistribute signaling molecules during cell fate determination (Hutterer and Knoblich, 2005; Kramer, 2000; Le Borgne, 2006; Parks et al., 2000). In yeast, endocytosis and plasma membrane recycling contribute to cell polarization (Valdez-Taubas and Pelham, 2003). Vesicle endocytosis and trafficking may also play a role in migration (Rosse et al., 2006; Sheen et al., 2004). Real-time imaging detected endocytic markers (eg. clathrin and dynamin) that are polarized toward and localized at the leading edge of migrating cells (Rappoport and Simon, 2003). In mammary carcinoma cells, an epidermal growth factor (EGF) gradient leads to the accumulation of endocytosed EGF receptors on the side of the cell facing the EGF source. In migrating neural precursors, vesicles accumulate in the leading process (Schaar and McConnell, 2005). Genetic studies in Drosophila indicate that mutation of the ubiquitin-ligase D-cbl leads to impaired migration of border cells during oocytogenesis. This mutation attenuates EGF-receptor ubiquitination and so alters receptor endocytosis and signaling (Jekely et al., 2005). We now show that BDNF-induced initiation and directionality of migration are both abrogated by endocytosis inhibitors, but these agents do not affect GCP migration in the absence of BDNF. Thus, endocytosis of TrkB receptors is needed for BDNF-induced chemotaxis.

Our data indicate that correct localization as well as formation of TrkB-containing signaling endosomes are required for BDNF-induced chemotaxis. Vesicles containing TrkB preferentially accumulate at the front of wild type GCPs when they are stimulated to chemotax by a gradient of BDNF. In contrast, when wild type GCPs are stimulated with uniformly distributed BDNF, TrkB-containing vesicles are oriented in any direction, and the cells migrate with arbitrary directionality. Strikingly, in GCPs prepared from *bdnf−/−* mice and stimulated either by a BDNF gradient or by uniformly distributed BDNF, TrkB containing vesicles are also oriented in multiple directions. In this genetic model, arbitrary localization of receptors is associated with random direction of migration. We conclude that both formation and localization of signaling endosomes are important for correct cell polarization and directional migration of GCPs in response to a BDNF gradient, and that this provides a second mechanism allowing amplification of the chemotactic gradient.

We find that PI3 kinase activation and Tiam1-mediated activation of Rac are additional critical components of the migratory response to BDNF. Localization of activated TrkB, PIP3 phospholipids, and Tiam1 to signaling endosomes ensures that the polarity of cytoskeletal changes mediated by Rac and by phospholipids are coordinated, so that both designate the same directionality. As proposed in the local coupling model for directed chemotaxis (Arrieumerlou and Meyer, 2005), we suggest that these cytoskeletal rearrangements cumulatively differentiate the front from the back of the cell. Because activated TrkB receptors and downstream molecules are in signaling endosomes directed toward the source of the gradient, the cell reliably moves forward toward the BDNF source. *In vivo*, this insures directed movement of GCPs from the EGL toward the IGL.

Together, the findings here suggest the following model for BDNF regulation of directed migration of GCPs. As GCPs mature, they increase expression of BDNF (Maisonpierre et al., 1990). Therefore the mature granule cells that have reached the IGL produce BDNF that disperses through the cerebellar cortex, forming an extracellular gradient from the IGL toward the EGL. This BDNF gradient stimulates TrkB receptors of GCPs that are poised to migrate. In turn, activated TrkB receptors of these precursors initiate autocrine release of BDNF, amplifying the ligand gradient and also causing further TrkB activation and endocytosis. Localized endocytosis of activated TrkB results in accumulation of signaling endosomes at the cellular location where BDNF is maximal, polarizing the cell through the actions of Rac and PIP3 phospholipids. Thus, autocrine release of BDNF and localized accumulation of signaling endosomes amplify the chemotactic gradient and correctly polarize the cell for directed migration.

Experimental Procedures

Animals

Breeding pairs of brain-derived neurotrophic factor *bdnf* +/− mice (Ernfors et al., 1994), C57BL/6-Tg (ACTB-EGFP)1Osb/J mice expressing EGFP (Okabe et al., 1997) and p75NTR +/− (exon III) mice (Lee et al., 1992) were purchased from the Jackson Laboratory (Bar Harbor, ME). BALB/c mouse breeding pairs were purchased from Charles River Laboratories (Wilmington, MA). All experimental procedures were performed in accordance with the National Institutes of Health guidelines and were approved by the Dana-Farber Cancer Institutional Animal Care and Use Committee.

Antibodies and Pharmacological Reagents

The antibodies and pharmacological reagents used were described in the Supplemental Data.

DNA Constructs and Lentivirus Production

The lentivirus construct expressing Tiam1 siRNA was described previously (Tolias et al., 2005). The lentivirus constructs expressing *bdnf* siRNA, wild type and K44A mutant dynamin are described in the Supplemental Data. Lentivirus was generated as described previously (Rubinson et al., 2003). Viral titers were determined by infection of HEK 293T cells (ATCC).

Primary Granule Cell and Glia Cell Culture

Primary cultures of granule cell precursors (GCPs) from P4 or P6 mouse cerebella were prepared as described previously (Choi et al., 2005; Klein et al., 2001). See the Supplemental Data for details.

Lentiviral Infection of Primary Cerebellar Granule Cells

Dissociated GCPs from P4 mice were directly resuspended in virus-containing N2 medium with 0.4 μg/ml poly-brene (Sigma), plated at high density ($2–4 \times 10^6$ cell/ml) in an uncoated 6-well tissue culture plate overnight and then changed to fresh N2 medium supplemented with 2 ug/ml SHH. Forty eight hours later, aggregate cultures were dissociated with papain dissociation kit (Worthington Biochemical Co., Lakewood, New Jersey) according to the manufacturer's instructions, then used for biochemical assays or real-time migration assay. Infection efficiency of GCPs with lentivirus is 80% on average, determined by the percentage of GFP-positive cells.

Organotypic Slice Culture, BrdU Labeling, Viral Infection and Immunostaining

Organotyptic cerebellar slices were prepared as described previously (Choi et al., 2005; Stoppini et al., 1991). See the Supplemental Data for details on slice culture, BrdU labeling, viral infection and immunostaing.

Immunoprecipitations and Western Blot Analysis

See the Supplemental Data for details on immunoprecipitations and Western blotting.

Determination of BDNF Concentration

BDNF concentrations were determined by ELISA using BDNF $E_{max}^{®}$ ImmunoAssay system (Promega). See the Supplemental Data for details.

Rac1, cdc42, RhoA Activation Assay and Evaluation of Surface TrkB Internalization

TrkB internalization was evaluated by biotinylation of surface TrkB with EZ-Link® Sulfo-NHS-biotin (Pierce). Rac1, RhoA and cdc42 activation were assessed by GST-PBD and GST-RBD pull-down assay kit (UBI). See the Supplemental Data for details.

Immunocytochemistry, Immunohistochemistry and Image Analysis

Immunocytochemistry, immunohistochemistry and image analysis were carried out using standard protocols. See the Supplemental Data for details.

Real-time Migration Assay

GCPs were prepared and plated as described above. Four hours after plating, a gradient of BDNF was created by loading 2 μg of BDNF to 50 μl of 1% agarose gel (Invitrogen) glued to one side of the 35 mm tissue culture dish (see Figure 1B). After plating, cells were observed under an inverted microscope Zeiss Axiovert 200 M, in bright field, and images were captured using a Photometrics CoolSNAP HQ digital camera controlled by Slidebook software (Intelligent Imaging Innovations, Inc). For assays using a source of BDNF in the agarose, the dishes were incubated for 4 hours at 37°C to allow diffusion of BDNF. One field close to the agarose was selected for observation and pictures were taken every 2 min during 2 hours. The pictures were then transferred to Adobe Photoshop, and the total number of cells and number of migrating cells were determined. The parameters measured were the following: 1) percentage of cells that migrate; 2) speed of migration (μm/h); and 3) direction of migration, classified as toward or away from the BDNF source.

On Adobe Photoshop 7.0, individual images were compiled as layers, the movement of single granule cells was traced, and the parameters of cell speed (μm/hour) and direction (toward or away from the plug) were determined. To compute the percentage of cells that migrate, the number of migrating granule cells was divided by the total isolated granule cells (both migrating and non-migrating) in the field and multiplied by 100. In each experiment, the percentage obtained from the condition without BDNF was assigned a value of 100% and all other conditions (i.e. gradient BDNF and uniform BDNF) were measured relative to this basal condition. To calculate the percentage of cells migrating toward versus away from the BDNF source, all cells that migrated in the upward direction relative to the horizontal (pictures were taken such that the agarose plug was at the top of the field) were counted as migrating “toward” whereas any cells that moved in the downward direction were counted as “away.” Because the BDNF-containing plug is smaller than the width of the microscope field, cells migrating toward the source appear to travel at an angle of 0–45 degrees relative to the y- axis, and so further parsing of directionality is not helpful.

To calculate standard errors in results pooled from multiple experiments (each graph represents the mean of 3–4 individual experiments) we used two methods. In the first method, for each individual experiment we normalized the percent of migrating cells and the percent of cells migrating toward or away under each condition to the values obtained in that experiment with no BDNF and no other intervention. Thus, control values are 100% by definition. Standard deviations for migration were calculated for each condition, and used to generate standard error of the mean. When we compare migration in cells from mutant and wild type animals, where there are two distinct cell preparations in each experiment, we calculated standard deviation by designating the migratory index of each cell as 0 for a non-migrating cell, and 1 for a migrating cell. Standard deviations and standard errors for migratory indices of the cells from all three experiments were then calculated for each condition.

Calculations for the random migration coefficient (μ) were based on the algorithm presented by Shreiber and colleagues (Shreiber et al., 2003). To quantify cell migration, the mean-squared

displacement $<d^2(t)>$ is calculated from position data over all experimental time, ultimately yielding a single value for the random cell migration coefficient μ, that describes the average migration of the population of cells over the duration of the experiment. Then, $<d^2(t)>$ is fit to a persistent random walk model with a GLSR algorithm. Any cell that moved faster than 150 μm/hour was excluded because it was presumed to be a dead or floating cell.

Supplementary Material

Refer to Web version on PubMed Central for supplementary material.

Acknowledgements

We would like to thank Erin Berry for technical assistance, Louis F. Reichardt for the generous gift of TrkB antibody. We thank Joshua Rubin, Aymeric Hans, Jennifer Chan, Kellie Nazemi, Stephanie Courchesne, Rochelle Witt and Charles Stiles for helpful suggestions. This work was supported by grants from the NIH (NS377057 to RAS and NS045500 to MEG), the Lefler Foundation (to MP and RAS), the Trudy Bettiker/American Brain Tumor Association Fellowship (to PZ) and the Children's Hospital Boston Mental Retardation and Developmental Disabilities Research Center, P01 HD18655.

References

Affolter M, Weijer CJ. Signaling to cytoskeletal dynamics during chemotaxis. Dev Cell 2005;9:19–34. [PubMed: 15992538]

Arrieumerlou C, Meyer T. A local coupling model and compass parameter for eukaryotic chemotaxis. Dev Cell 2005;8:215–227. [PubMed: 15691763]

Aruga J, Yokota N, Hashimoto M, Furuichi T, Fukuda M, Mikoshiba K. A novel zinc finger protein, zic, is involved in neurogenesis, especially in the cell lineage of cerebellar granule cells. J Neurochem 1994;63:1880–1890. [PubMed: 7931345]

Bagnard D, Vaillant C, Khuth ST, Dufay N, Lohrum M, Puschel AW, Belin MF, Bolz J, Thomasset N. Semaphorin 3A-vascular endothelial growth factor-165 balance mediates migration and apoptosis of neural progenitor cells by the recruitment of shared receptor. J Neurosci 2001;21:3332–3341. [PubMed: 11331362]

Beattie EC, Zhou J, Grimes ML, Bunnett NW, Howe CL, Mobley WC. A signaling endosome hypothesis to explain NGF actions: potential implications for neurodegeneration. Cold Spring Harb Symp Quant Biol 1996;61:389–406. [PubMed: 9246468]

Bellion A, Baudoin JP, Alvarez C, Bornens M, Metin C. Nucleokinesis in tangentially migrating neurons comprises two alternating phases: forward migration of the Golgi/centrosome associated with centrosome splitting and myosin contraction at the rear. J Neurosci 2005;25:5691–5699. [PubMed: 15958735]

Bentley CA, Lee KF. p75 is important for axon growth and schwann cell migration during development. J Neurosci 2000;20:7706–7715. [PubMed: 11027232]

Bielas SL, Gleeson JG. Cytoskeletal-associated proteins in the migration of cortical neurons. J Neurobiol 2004;58:149–159. [PubMed: 14598377]

Bloch-Gallego E, Ezan F, Tessier-Lavigne M, Sotelo C. Floor plate and netrin-1 are involved in the migration and survival of inferior olivary neurons. J Neurosci 1999;19:4407–4420. [PubMed: 10341242]

Bokoch GM, Vlahos CJ, Wang Y, Knaus UG, Traynor-Kaplan AE. Rac GTPase interacts specifically with phosphatidylinositol 3-kinase. Biochem J 1996;315(Pt 3):775–779. [PubMed: 8645157]

Borghesani PR, Peyrin JM, Klein R, Rubin J, Carter AR, Schwartz PM, Luster A, Corfas G, Segal RA. BDNF stimulates migration of cerebellar granule cells. Development 2002;129:1435–1442. [PubMed: 11880352]

Brose K, Tessier-Lavigne M. Slit proteins: key regulators of axon guidance, axonal branching, and cell migration. Curr Opin Neurobiol 2000;10:95–102. [PubMed: 10679444]

Burke P, Schooler K, Wiley HS. Regulation of epidermal growth factor receptor signaling by endocytosis and intracellular trafficking. Mol Biol Cell 2001;12:1897–1910. [PubMed: 11408594]

Canossa M, Griesbeck O, Berninger B, Campana G, Kolbeck R, Thoenen H. Neurotrophin release by neurotrophins: implications for activity-dependent neuronal plasticity. Proc Natl Acad Sci U S A 1997;94:13279–13286. [PubMed: 9371837]

Carter AR, Berry EM, Segal RA. Regional expression of p75NTR contributes to neurotrophin regulation of cerebellar patterning. Mol Cell Neurosci 2003;22:1–13. [PubMed: 12595234]

Choi Y, Borghesani PR, Chan JA, Segal RA. Migration from a mitogenic niche promotes cell-cycle exit. J Neurosci 2005;25:10437–10445. [PubMed: 16280582]

Conover JC, Doetsch F, Garcia-Verdugo JM, Gale NW, Yancopoulos GD, Alvarez-Buylla A. Disruption of Eph/ephrin signaling affects migration and proliferation in the adult subventricular zone. Nat Neurosci 2000;3:1091–1097. [PubMed: 11036265]

Damke H, Baba T, Warnock DE, Schmid SL. Induction of mutant dynamin specifically blocks endocytic coated vesicle formation. J Cell Biol 1994;127:915–934. [PubMed: 7962076]

Davies PJ, Davies DR, Levitzki A, Maxfield FR, Milhaud P, Willingham MC, Pastan IH. Transglutaminase is essential in receptor-mediated endocytosis of alpha 2-macroglobulin and polypeptide hormones. Nature 1980;283:162–167. [PubMed: 6153122]

Di Fiore PP, De Camilli P. Endocytosis and signaling. an inseparable partnership. Cell 2001;106:1–4. [PubMed: 11461694]

Dujardin DL, Barnhart LE, Stehman SA, Gomes ER, Gundersen GG, Vallee RB. A role for cytoplasmic dynein and LIS1 in directed cell movement. J Cell Biol 2003;163:1205–1211. [PubMed: 14691133]

Edmondson JC, Hatten ME. Glial-guided granule neuron migration in vitro: a high-resolution time-lapse video microscopic study. J Neurosci 1987;7:1928–1934. [PubMed: 3598656]

Ehler E, van Leeuwen F, Collard JG, Salinas PC. Expression of Tiam-1 in the developing brain suggests a role for the Tiam-1-Rac signaling pathway in cell migration and neurite outgrowth. Mol Cell Neurosci 1997;9:1–12. [PubMed: 9204476]

Ernfors P, Lee KF, Jaenisch R. Mice lacking brain-derived neurotrophic factor develop with sensory deficits. Nature 1994;368:147–150. [PubMed: 8139657]

Fishell G, Hatten ME. Astrotactin provides a receptor system for CNS neuronal migration. Development 1991;113:755–765. [PubMed: 1821847]

Funamoto S, Meili R, Lee S, Parry L, Firtel RA. Spatial and temporal regulation of 3-phosphoinositides by PI 3-kinase and PTEN mediates chemotaxis. Cell 2002;109:611–623. [PubMed: 12062104]

Gammill LS, Gonzalez C, Gu C, Bronner-Fraser M. Guidance of trunk neural crest migration requires neuropilin 2/semaphorin 3F signaling. Development 2006;133:99–106. [PubMed: 16319111]

Ginty DD, Segal RA. Retrograde neurotrophin signaling: Trk-ing along the axon. Curr Opin Neurobiol 2002;12:268–274. [PubMed: 12049932]

Gonzalez-Gaitan M, Jackle H. Role of Drosophila alpha-adaptin in presynaptic vesicle recycling. Cell 1997;88:767–776. [PubMed: 9118220]

Grimes ML, Zhou J, Beattie EC, Yuen EC, Hall DE, Valletta JS, Topp KS, LaVail JH, Bunnett NW, Mobley WC. Endocytosis of activated TrkA: evidence that nerve growth factor induces formation of signaling endosomes. J Neurosci 1996;16:7950–7964. [PubMed: 8987823]

Hamasaki T, Goto S, Nishikawa S, Ushio Y. A role of netrin-1 in the formation of the subcortical structure striatum: repulsive action on the migration of late-born striatal neurons. J Neurosci 2001;21:4272–4280. [PubMed: 11404412]

Hatten ME. Central nervous system neuronal migration. Annu Rev Neurosci 1999;22:511–539. [PubMed: 10202547]

Hatten ME. New directions in neuronal migration. Science 2002;297:1660–1663. [PubMed: 12215636]

Hawkins PT, Eguinoa A, Qiu RG, Stokoe D, Cooke FT, Walters R, Wennstrom S, Claesson-Welsh L, Evans T, Symons M, et al. PDGF stimulates an increase in GTP-Rac via activation of phosphoinositide 3-kinase. Curr Biol 1995;5:393–403. [PubMed: 7627555]

Heerssen HM, Pazyra MF, Segal RA. Dynein motors transport activated Trks to promote survival of target-dependent neurons. Nat Neurosci 2004;7:596–604. [PubMed: 15122257]

Howe CL. Modeling the signaling endosome hypothesis: why a drive to the nucleus is better than a (random) walk. Theor Biol Med Model 2005;2:43. [PubMed: 16236165]

Howe CL, Mobley WC. Signaling endosome hypothesis: A cellular mechanism for long distance communication. J Neurobiol 2004;58:207–216. [PubMed: 14704953]

Huang C, Jacobson K, Schaller MD. MAP kinases and cell migration. J Cell Sci 2004;117:4619–4628. [PubMed: 15371522]

Huang EJ, Reichardt LF. Trk receptors: roles in neuronal signal transduction. Annu Rev Biochem 2003;72:609–642. [PubMed: 12676795]

Hutterer A, Knoblich JA. Numb and alpha-Adaptin regulate Sanpodo endocytosis to specify cell fate in Drosophila external sensory organs. EMBO Rep 2005;6:836–842. [PubMed: 16113648]

Iijima M, Huang YE, Devreotes P. Temporal and spatial regulation of chemotaxis. Dev Cell 2002;3:469–478. [PubMed: 12408799]

Jekely G, Sung HH, Luque CM, Rorth P. Regulators of endocytosis maintain localized receptor tyrosine kinase signaling in guided migration. Dev Cell 2005;9:197–207. [PubMed: 16054027]

Jones KR, Farinas I, Backus C, Reichardt LF. Targeted disruption of the BDNF gene perturbs brain and sensory neuron development but not motor neuron development. Cell 1994;76:989–999. [PubMed: 8137432]

Keely PJ, Westwick JK, Whitehead IP, Der CJ, Parise LV. Cdc42 and Rac1 induce integrin-mediated cell motility and invasiveness through PI(3)K. Nature 1997;390:632–636. [PubMed: 9403696]

Kerjan G, Dolan J, Haumaitre C, Schneider-Maunoury S, Fujisawa H, Mitchell KJ, Chedotal A. The transmembrane semaphorin Sema6A controls cerebellar granule cell migration. Nat Neurosci 2005;8:1516–1524. [PubMed: 16205717]

Klein R, Martin-Zanca D, Barbacid M, Parada LF. Expression of the tyrosine kinase receptor gene trkB is confined to the murine embryonic and adult nervous system. Development 1990;109:845–850. [PubMed: 2171894]

Klein RS, Rubin JB, Gibson HD, DeHaan EN, Alvarez-Hernandez X, Segal RA, Luster AD. SDF-1 alpha induces chemotaxis and enhances Sonic hedgehog-induced proliferation of cerebellar granule cells. Development 2001;128:1971–1981. [PubMed: 11493520]

Komuro H, Rakic P. Modulation of neuronal migration by NMDA receptors. Science 1993;260:95–97. [PubMed: 8096653]

Komuro H, Yacubova E. Recent advances in cerebellar granule cell migration. Cell Mol Life Sci 2003;60:1084–1098. [PubMed: 12861377]

Komuro H, Yacubova E, Rakic P. Mode and tempo of tangential cell migration in the cerebellar external granular layer. J Neurosci 2001;21:527–540. [PubMed: 11160432]

Kramer H. RIPping notch apart: a new role for endocytosis in signal transduction? Sci STKE 2000;2000:PE1. [PubMed: 11752592]

Kramer SG, Kidd T, Simpson JH, Goodman CS. Switching repulsion to attraction: changing responses to slit during transition in mesoderm migration. Science 2001;292:737–740. [PubMed: 11326102]

Kruttgen A, Moller JC, Heymach JV Jr, Shooter EM. Neurotrophins induce release of neurotrophins by the regulated secretory pathway. Proc Natl Acad Sci U S A 1998;95:9614–9619. [PubMed: 9689129]

Lambert JM, Lambert QT, Reuther GW, Malliri A, Siderovski DP, Sondek J, Collard JG, Der CJ. Tiam1 mediates Ras activation of Rac by a PI(3)K-independent mechanism. Nat Cell Biol 2002;4:621–625. [PubMed: 12134164]

Lambert WS, Clark AF, Wordinger RJ. Effect of exogenous neurotrophins on Trk receptor phosphorylation, cell proliferation, and neurotrophin secretion by cells isolated from the human lamina cribrosa. Mol Vis 2004;10:289–296. [PubMed: 15105791]

Le Borgne R. Regulation of Notch signalling by endocytosis and endosomal sorting. Curr Opin Cell Biol 2006;18:213–222. [PubMed: 16488590]

Le Roy C, Wrana JL. Signaling and endocytosis: a team effort for cell migration. Dev Cell 2005;9:167–168. [PubMed: 16054022]

Lee KF, Li E, Huber LJ, Landis SC, Sharpe AH, Chao MV, Jaenisch R. Targeted mutation of the gene encoding the low affinity NGF receptor p75 leads to deficits in the peripheral sensory nervous system. Cell 1992;69:737–749. [PubMed: 1317267]

Lu Q, Sun EE, Klein RS, Flanagan JG. Ephrin-B reverse signaling is mediated by a novel PDZ-RGS protein and selectively inhibits G protein-coupled chemoattraction. Cell 2001;105:69–79. [PubMed: 11301003]

Maisonpierre PC, Belluscio L, Friedman B, Alderson RF, Wiegand SJ, Furth ME, Lindsay RM, Yancopoulos GD. NT-3, BDNF, and NGF in the developing rat nervous system: parallel as well as reciprocal patterns of expression. Neuron 1990;5:501–509. [PubMed: 1688327]

Medina DL, Sciarretta C, Calella AM, Von Bohlen Und Halbach O, Unsicker K, Minichiello L. TrkB regulates neocortex formation through the Shc/PLCgamma-mediated control of neuronal migration. Embo J 2004;23:3803–3814. [PubMed: 15372074]

Merlot S, Firtel RA. Leading the way: Directional sensing through phosphatidylinositol 3-kinase and other signaling pathways. J Cell Sci 2003;116:3471–3478. [PubMed: 12893811]

Mertens AE, Roovers RC, Collard JG. Regulation of Tiam1-Rac signalling. FEBS Lett 2003;546:11–16. [PubMed: 12829230]

Minichiello L, Casagranda F, Tatche RS, Stucky CL, Postigo A, Lewin GR, Davies AM, Klein R. Point mutation in trkB causes loss of NT4-dependent neurons without major effects on diverse BDNF responses. Neuron 1998;21:335–345. [PubMed: 9728915]

Minichiello L, Klein R. TrkB and TrkC neurotrophin receptors cooperate in promoting survival of hippocampal and cerebellar granule neurons. Genes Dev 1996;10:2849–2858. [PubMed: 8918886]

Miyamoto Y, Yamauchi J, Tanoue A, Wu C, Mobley WC. TrkB binds and tyrosine-phosphorylates Tiam1, leading to activation of Rac1 and induction of changes in cellular morphology. Proc Natl Acad Sci U S A 2006;103:10444–10449. [PubMed: 16801538]

Myers SA, Han JW, Lee Y, Firtel RA, Chung CY. A Dictyostelium homologue of WASP is required for polarized F-actin assembly during chemotaxis. Mol Biol Cell 2005;16:2191–2206. [PubMed: 15728724]

Nadarajah B, Alifragis P, Wong RO, Parnavelas JG. Ventricle-directed migration in the developing cerebral cortex. Nat Neurosci 2002;5:218–224. [PubMed: 11850632]

Nadarajah B, Brunstrom JE, Grutzendler J, Wong RO, Pearlman AL. Two modes of radial migration in early development of the cerebral cortex. Nat Neurosci 2001;4:143–150. [PubMed: 11175874]

Nadarajah B, Parnavelas JG. Modes of neuronal migration in the developing cerebral cortex. Nat Rev Neurosci 2002;3:423–432. [PubMed: 12042877]

Nagano T, Morikubo S, Sato M. Filamin A and FILIP (Filamin A-Interacting Protein) regulate cell polarity and motility in neocortical subventricular and intermediate zones during radial migration. J Neurosci 2004;24:9648–9657. [PubMed: 15509752]

Nagano T, Yoneda T, Hatanaka Y, Kubota C, Murakami F, Sato M. Filamin A-interacting protein (FILIP) regulates cortical cell migration out of the ventricular zone. Nat Cell Biol 2002;4:495–501. [PubMed: 12055638]

Okabe M, Ikawa M, Kominami K, Nakanishi T, Nishimune Y. 'Green mice' as a source of ubiquitous green cells. FEBS Lett 1997;407:313–319. [PubMed: 9175875]

Parks AL, Klueg KM, Stout JR, Muskavitch MA. Ligand endocytosis drives receptor dissociation and activation in the Notch pathway. Development 2000;127:1373–1385. [PubMed: 10704384]

Piper M, Little M. Movement through Slits: cellular migration via the Slit family. Bioessays 2003;25:32–38. [PubMed: 12508280]

Polleux F, Whitford KL, Dijkhuizen PA, Vitalis T, Ghosh A. Control of cortical interneuron migration by neurotrophins and PI3-kinase signaling. Development 2002;129:3147–3160. [PubMed: 12070090]

Qi M, Ikematsu S, Maeda N, Ichihara-Tanaka K, Sakuma S, Noda M, Muramatsu T, Kadomatsu K. Haptotactic migration induced by midkine. Involvement of protein-tyrosine phosphatase zeta. Mitogen-activated protein kinase, and phosphatidylinositol 3-kinase. J Biol Chem 2001;276:15868–15875. [PubMed: 11340082]

Qin J, Mizuguchi M, Itoh M, Takashima S. A novel migration-related gene product, doublecortin, in neuronal migration disorder of fetuses and infants with Zellweger syndrome. Acta Neuropathol (Berl) 2000;100:168–173. [PubMed: 10963364]

Raftopoulou M, Hall A. Cell migration: Rho GTPases lead the way. Dev Biol 2004;265:23–32. [PubMed: 14697350]

Rakic P. Neuron-glia relationship during granule cell migration in developing cerebellar cortex. A Golgi and electronmicroscopic study in Macacus Rhesus. J Comp Neurol 1971;141:283–312. [PubMed: 4101340]

Rappoport JZ, Simon SM. Real-time analysis of clathrin-mediated endocytosis during cell migration. J Cell Sci 2003;116:847–855. [PubMed: 12571282]

Ridley AJ, Schwartz MA, Burridge K, Firtel RA, Ginsberg MH, Borisy G, Parsons JT, Horwitz AR. Cell migration: integrating signals from front to back. Science 2003;302:1704–1709. [PubMed: 14657486]

Ringstedt T, Linnarsson S, Wagner J, Lendahl U, Kokaia Z, Arenas E, Ernfors P, Ibanez CF. BDNF regulates reelin expression and Cajal-Retzius cell development in the cerebral cortex. Neuron 1998;21:305–315. [PubMed: 9728912]

Rio C, Rieff HI, Qi P, Khurana TS, Corfas G. Neuregulin and erbB receptors play a critical role in neuronal migration. Neuron 1997;19:39–50. [PubMed: 9247262]

Rivas RJ, Hatten ME. Motility and cytoskeletal organization of migrating cerebellar granule neurons. J Neurosci 1995;15:981–989. [PubMed: 7869123]

Robinson MS. The role of clathrin, adaptors and dynamin in endocytosis. Curr Opin Cell Biol 1994;6:538–544. [PubMed: 7986531]

Rocamora N, Garcia-Ladona FJ, Palacios JM, Mengod G. Differential expression of brain-derived neurotrophic factor, neurotrophin-3, and low-affinity nerve growth factor receptor during the postnatal development of the rat cerebellar system. Brain Res Mol Brain Res 1993;17:1–8. [PubMed: 8381892]

Rosse C, Hatzoglou A, Parrini MC, White MA, Chavrier P, Camonis J. RalB mobilizes the exocyst to drive cell migration. Mol Cell Biol 2006;26:727–734. [PubMed: 16382162]

Rubinson DA, Dillon CP, Kwiatkowski AV, Sievers C, Yang L, Kopinja J, Rooney DL, Ihrig MM, McManus MT, Gertler FB, et al. A lentivirus-based system to functionally silence genes in primary mammalian cells, stem cells and transgenic mice by RNA interference. Nat Genet 2003;33:401–406. [PubMed: 12590264]

Saarelainen T, Vaittinen S, Castren E. trkB-receptor activation contributes to the kainate-induced increase in BDNF mRNA synthesis. Cellular and molecular neurobiology 2001;21:429–435. [PubMed: 11775072]

Sadakata T, Kakegawa W, Mizoguchi A, Washida M, Katoh-Semba R, Shutoh F, Okamoto T, Nakashima H, Kimura K, Tanaka M, et al. Impaired cerebellar development and function in mice lacking CAPS2, a protein involved in neurotrophin release. J Neurosci 2007;27:2472–2482. [PubMed: 17344385]

Sadakata T, Mizoguchi A, Sato Y, Katoh-Semba R, Fukuda M, Mikoshiba K, Furuichi T. The secretory granule-associated protein CAPS2 regulates neurotrophin release and cell survival. J Neurosci 2004;24:43–52. [PubMed: 14715936]

Sander EE, van Delft S, ten Klooster JP, Reid T, van der Kammen RA, Michiels F, Collard JG. Matrix-dependent Tiam1/Rac signaling in epithelial cells promotes either cell-cell adhesion or cell migration and is regulated by phosphatidylinositol 3-kinase. J Cell Biol 1998;143:1385–1398. [PubMed: 9832565]

Santiago A, Erickson CA. Ephrin-B ligands play a dual role in the control of neural crest cell migration. Development 2002;129:3621–3632. [PubMed: 12117812]

Sawada J, Itakura A, Tanaka A, Furusaka T, Matsuda H. Nerve growth factor functions as a chemoattractant for mast cells through both mitogen-activated protein kinase and phosphatidylinositol 3-kinase signaling pathways. Blood 2000;95:2052–2058. [PubMed: 10706874]

Schaar BT, McConnell SK. Cytoskeletal coordination during neuronal migration. Proc Natl Acad Sci U S A 2005;102:13652–13657. [PubMed: 16174753]

Segal RA, Pomeroy SL, Stiles CD. Axonal growth and fasciculation linked to differential expression of BDNF and NT3 receptors in developing cerebellar granule cells. J Neurosci 1995;15:4970–4981. [PubMed: 7623126]

Servant G, Weiner OD, Herzmark P, Balla T, Sedat JW, Bourne HR. Polarization of chemoattractant receptor signaling during neutrophil chemotaxis. Science 2000;287:1037–1040. [PubMed: 10669415]

Sheen VL, Ganesh VS, Topcu M, Sebire G, Bodell A, Hill RS, Grant PE, Shugart YY, Imitola J, Khoury SJ, et al. Mutations in ARFGEF2 implicate vesicle trafficking in neural progenitor proliferation and migration in the human cerebral cortex. Nat Genet 2004;36:69–76. [PubMed: 14647276]

Shreiber DI, Barocas VH, Tranquillo RT. Temporal variations in cell migration and traction during fibroblast-mediated gel compaction. Biophys J 2003;84:4102–4114. [PubMed: 12770913]

Snapper SB, Meelu P, Nguyen D, Stockton BM, Bozza P, Alt FW, Rosen FS, von Andrian UH, Klein C. WASP deficiency leads to global defects of directed leukocyte migration in vitro and in vivo. J Leukoc Biol 2005;77:993–998. [PubMed: 15774550]

Stoppini L, Buchs PA, Muller D. A simple method for organotypic cultures of nervous tissue. J Neurosci Methods 1991;37:173–182. [PubMed: 1715499]

Takei K, Haucke V. Clathrin-mediated endocytosis: membrane factors pull the trigger. Trends Cell Biol 2001;11:385–391. [PubMed: 11514193]

Tolias KF, Bikoff JB, Burette A, Paradis S, Harrar D, Tavazoie S, Weinberg RJ, Greenberg ME. The Rac1-GEF Tiam1 couples the NMDA receptor to the activity-dependent development of dendritic arbors and spines. Neuron 2005;45:525–538. [PubMed: 15721239]

Tolias KF, Cantley LC, Carpenter CL. Rho family GTPases bind to phosphoinositide kinases. J Biol Chem 1995;270:17656–17659. [PubMed: 7629060]

Tomoda T, Kim JH, Zhan C, Hatten ME. Role of Unc51.1 and its binding partners in CNS axon outgrowth. Genes Dev 2004;18:541–558. [PubMed: 15014045]

Tsai LH, Gleeson JG. Nucleokinesis in neuronal migration. Neuron 2005;46:383–388. [PubMed: 15882636]

Valdez G, Akmentin W, Philippidou P, Kuruvilla R, Ginty DD, Halegoua S. Pincher-mediated macroendocytosis underlies retrograde signaling by neurotrophin receptors. J Neurosci 2005;25:5236–5247. [PubMed: 15917464]

Valdez-Taubas J, Pelham HR. Slow diffusion of proteins in the yeast plasma membrane allows polarity to be maintained by endocytic cycling. Curr Biol 2003;13:1636–1640. [PubMed: 13678596]

van der Bliek AM, Redelmeier TE, Damke H, Tisdale EJ, Meyerowitz EM, Schmid SL. Mutations in human dynamin block an intermediate stage in coated vesicle formation. J Cell Biol 1993;122:553–563. [PubMed: 8101525]

Vicente-Manzanares M, Webb DJ, Horwitz AR. Cell migration at a glance. J Cell Sci 2005;118:4917–4919. [PubMed: 16254237]

Webb DJ, Zhang H, Horwitz AF. Cell migration: an overview. Methods Mol Biol 2005;294:3–11. [PubMed: 15576900]

Wetmore C, Ernfors P, Persson H, Olson L. Localization of brain-derived neurotrophic factor mRNA to neurons in the brain by in situ hybridization. Exp Neurol 1990;109:141–152. [PubMed: 2379553]

Wu W, Wong K, Chen J, Jiang Z, Dupuis S, Wu JY, Rao Y. Directional guidance of neuronal migration in the olfactory system by the protein Slit. Nature 1999;400:331–336. [PubMed: 10432110]

Yamauchi J, Chan JR, Shooter EM. Neurotrophin 3 activation of TrkC induces Schwann cell migration through the c-Jun N-terminal kinase pathway. Proc Natl Acad Sci U S A 2003;100:14421–14426. [PubMed: 14614136]

Yang ZF, Ho DW, Lau CK, Tam KH, Lam CT, Poon RT, Fan ST. Platelet activation during tumor development, the potential role of BDNF-TrkB autocrine loop. Biochemical and biophysical research communications 2006;346:981–985. [PubMed: 16781670]

Yee KT, Simon HH, Tessier-Lavigne M, O'Leary DM. Extension of long leading processes and neuronal migration in the mammalian brain directed by the chemoattractant netrin-1. Neuron 1999;24:607–622. [PubMed: 10595513]

Yoshizawa M, Kawauchi T, Sone M, Nishimura YV, Terao M, Chihama K, Nabeshima Y, Hoshino M. Involvement of a Rac activator, P-Rex1, in neurotrophin-derived signaling and neuronal migration. J Neurosci 2005;25:4406–4419. [PubMed: 15858067]

Yuen EC, Mobley WC. Early BDNF, NT-3, and NT-4 signaling events. Exp Neurol 1999;159:297–308. [PubMed: 10486198]

Zhang Y, Moheban DB, Conway BR, Bhattacharyya A, Segal RA. Cell surface Trk receptors mediate NGF-induced survival while internalized receptors regulate NGF-induced differentiation. J Neurosci 2000;20:5671–5678. [PubMed: 10908605]

Zheng Y, Bagrodia S, Cerione RA. Activation of phosphoinositide 3-kinase activity by Cdc42Hs binding to p85. J Biol Chem 1994;269:18727–18730. [PubMed: 8034624]

Zhu Y, Yu T, Zhang XC, Nagasawa T, Wu JY, Rao Y. Role of the chemokine SDF-1 as the meningeal attractant for embryonic cerebellar neurons. Nat Neurosci 2002;5:719–720. [PubMed: 12080344]

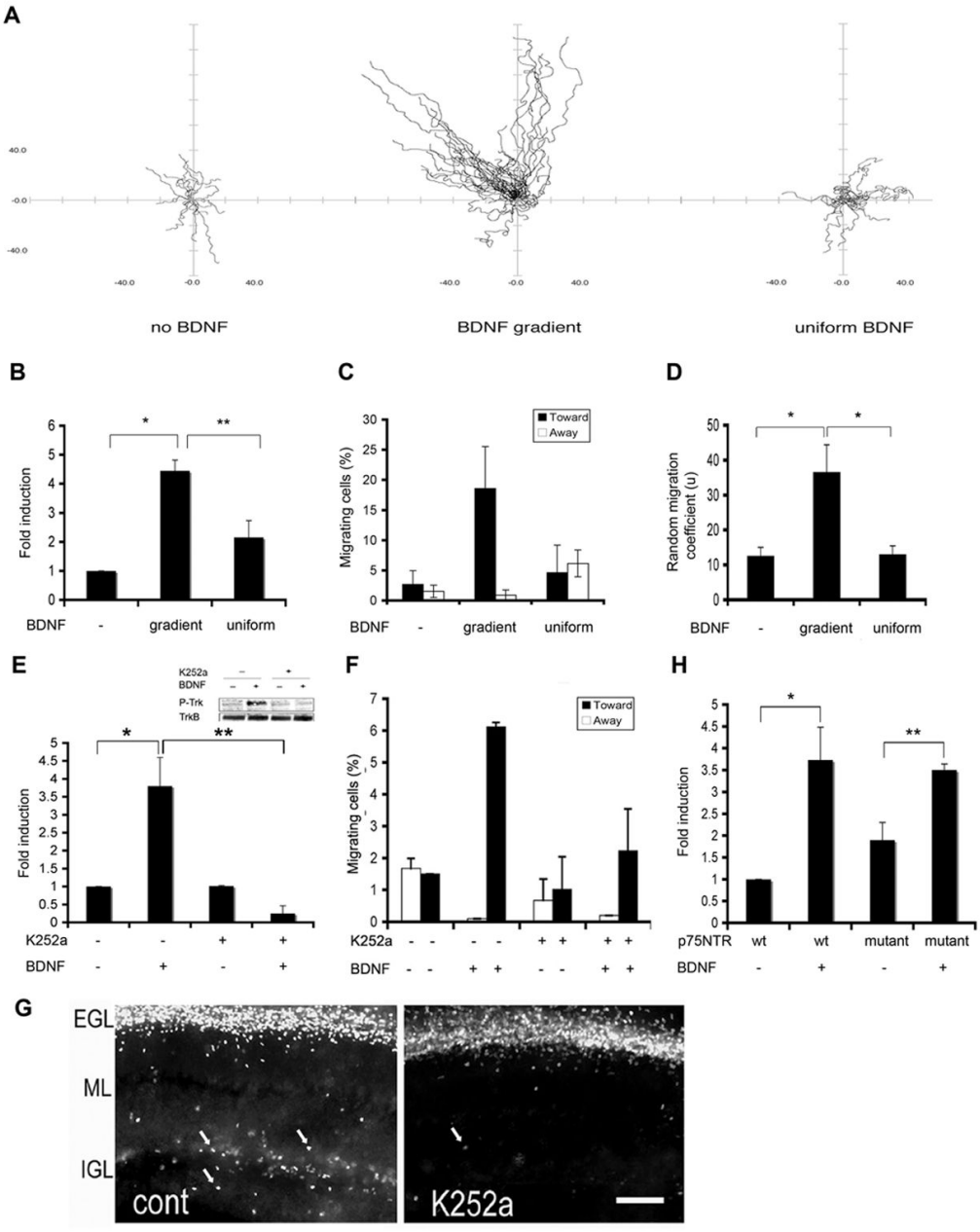

Figure 1. A Gradient of BDNF Promotes TrkB –dependent Chemotaxis of GCPs

(A) Pathway traces of individual migrating GCPs from four independent experiments for three conditions (no BDNF, gradient BDNF and uniform BDNF, respectively) were superimposed on a common origin. Because the BDNF-containing plug is smaller than the width of the microscope field, cells migrating toward the source travel at angles of 0–45 degrees relative to the y-axis, and fewer cells are precisely at 0 degrees.

(B) Quantitative analysis of GCP migration with no BDNF, gradient or uniform BDNF. Data represent mean of four independent experiments and were evaluated by z test (*, $p < 0.001$) and two-tailed Student's t test (**, $p < 0.05$), respectively.

(C) Quantitative analysis of directionality of GCP migration with no BDNF, gradient or uniform BDNF. Data shown represent means of four independent experiments ± SEM (n=4).

(D) Quantitative analysis of coefficient of non-randomness (μ) from the same experiments as A, B and C. Data were evaluated by two-tailed Student's t-test (*, $p < 0.001$).
(E) K252a, a Trk receptor inhibitor, blocks BDNF-induced GCP migration. Dissociated GCPs were exposed to a BDNF gradient in the absence or presence of 200 nM K252a. Data were evaluated by z test (*, $p < 0.001$) and two-tailed Student's t-test (**, $p < 0.001$), respectively.
(F) Quantitative analysis of directionality of GCP migration for experiments in 1E.
(G) K252a (200 nM) inhibits GCP migration in cultured organotypic cerebellar slices. Cerebellar slices (250μm) from P7 wild type mice were cultured in inserts and treated with K252a or vehicle control for 1 hour prior to BrdU pulse-labeling. After BrdU labeling, slices were cultured for additional for 72 hours, fixed with 4% paraformaldehyde and immunostained with anti-BrdU. The picture represents one sample of three independent experiments. Arrows indicate BrdU-positive GCPs in IGL. *Scale bar*: 100 μm.
(H) p75NTR is not required for BDNF-induced migration. Migration assay of dissociated GCPs from p75NTR wild type or exon III mutant littermates was carried out as described above. Data shown represent means ± SEM (n=3) and were evaluated by z test (*, $p < 0.05$) and by two-tailed Student's t-test ($p < 0.05$), respectively.

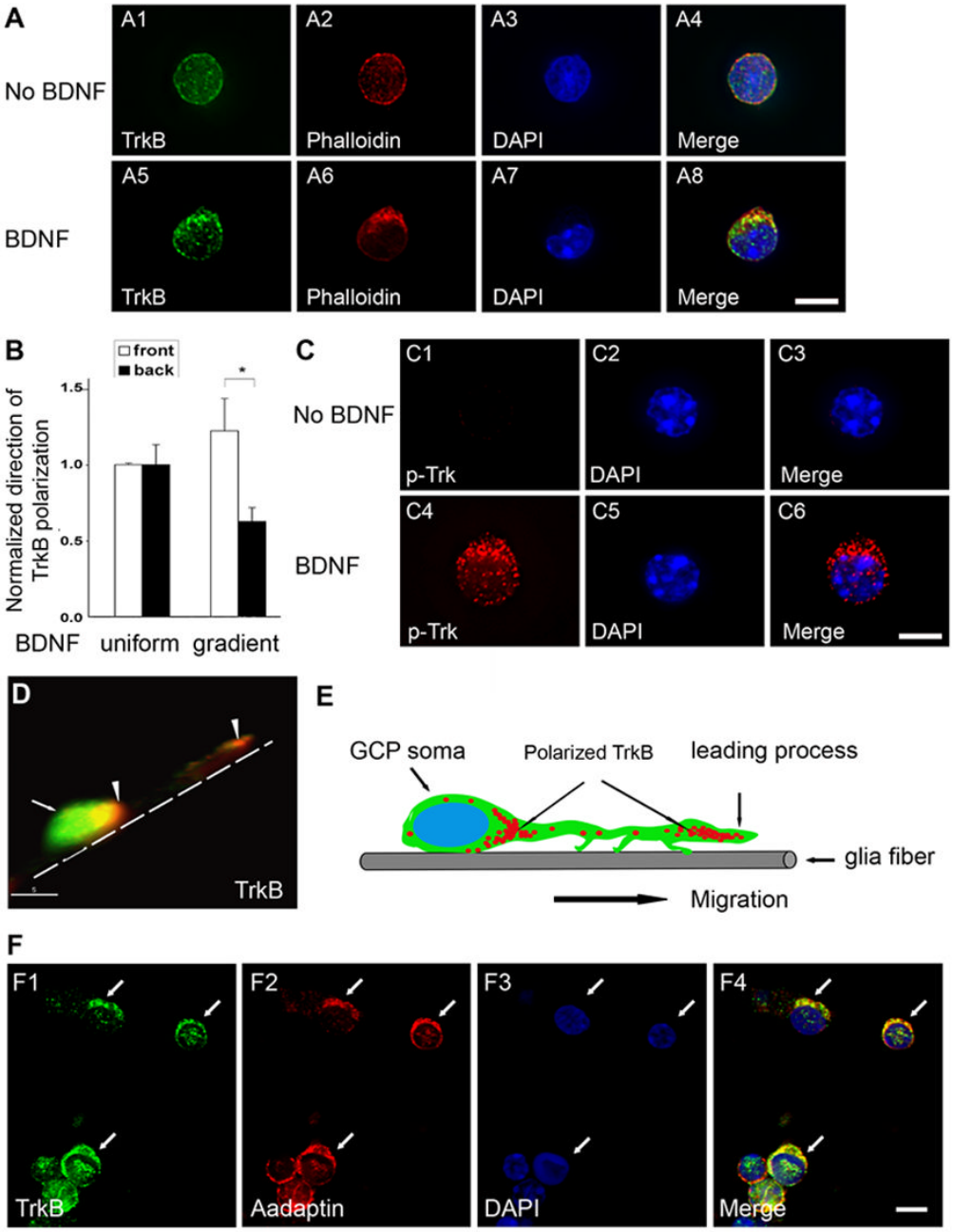

Figure 2. BDNF-dependent Polarization of TrkB Receptor in Cerebellar GCPs

GCPs grown on coverslips were or were not exposed to gradient BDNF for 12 hours, fixed and immunostained as indicated. In all cases, BDNF source is at the top. DAPI staining visualizes nuclei (blue). *Scale bars*: 5 μm.

(A) BDNF induces TrkB receptor and cytoskeletal polarization. F-actin cytoskeleton rearrangement was visualized by staining with Alexa®-568-phalloidin (red). Localization of TrkB receptor was visualized by immunofluorescent staining with anti-TrkB (green).

(B) Quantitative analysis of TrkB localization. GCPs were exposed to uniform or gradient BDNF for 12 hours, fixed and immunostained with TrkB antibody. TrkB localization in GCPs was assessed with fluorescent microscopy. In each of four experiments, the percentage of cells

with TrkB polarized toward the agarose plug (front) or away from the plug (back) was normalized to the percentage of cells with TrkB polarized to the front under uniform stimulation condition. Data shown represent means ± SEM (n=4) and were evaluated by two-tailed Student's t-test (*, $p < 0.01$).

(C) Polarized TrkB receptors at the front of the cell are activated, visualized by immunofluorescent staining with phospho-specific Trk antibody (red).

(D) BDNF-dependent polarization of TrkB receptors in GCPs migrating along glia fibers. Bergmann glia and GCPs were co-cultured for one day, treated with 10 ng/ml BDNF for 1 hour, then fixed and immunostained with anti-TrkB (red). A projection of three-dimensional reconstruction is shown. Broken line represents glia fiber. Arrow indicates the GCP soma (green) and arrowheads show polarized TrkB receptors at the front of soma (left) and in the leading process of GCP (right). *Scal bar*: 5 μm.

(E) Schematic of TrkB polarization in GCPs migrating along glia fiber in 2D. (F) Internalized TrkB receptors localize in early endosomal compartment. GCPs were exposed to gradient BDNF for 12 hours, then fixed and stained with anti-α-adaptin (red) and anti-TrkB (green). Arrow indicates polarized GCPs. BDNF source is on the top of the images. *Scale bar*: 5 μm.

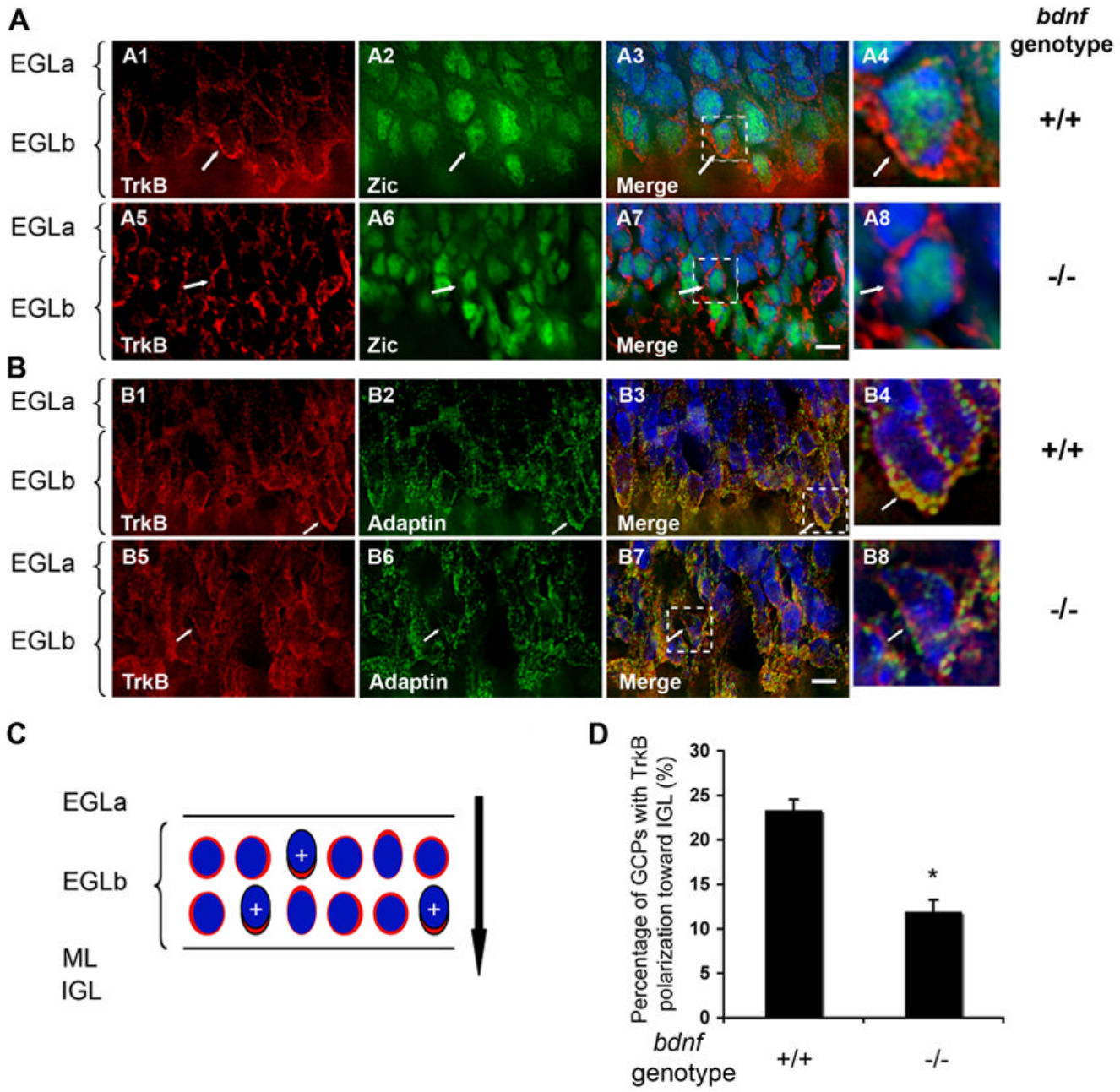

Figure 3. BDNF-dependent Formation and Polarization of TrkB Signaling Endosome *in vivo*

Cerebellar sections from P6 *bdnf* +/+ or −/− mice were used for immunostaining as indicated (A and B). DAPI staining visualizes nuclei (blue). Scale bars: 5 μm.

(A) BDNF-dependent polarization of TrkB receptors *in vivo*. TrkB receptors at the front of GCPs in EGLb are seen within a crescent or extended leading process in *bdnf* +/+ mice (A1–A4), but are more randomly distributed within the cells of *bdnf* −/− mice (A5–A8), as visualized by immunostaining with anti-TrkB (red) and anti-zic (green). A4 and A8 are magnified view of boxed region in A3 and A7, respectively.

(B) BDNF-dependent formation and polarization of TrkB signaling endosomes *in vivo*. TrkB receptors colocalize with α-adaptin at leading edge of GCPs from *bdnf* +/+ mice (B1–B4), but

are distributed in random patterns in *bdnf* −/− GCPs (B5–B8). Colocalization and polarization of TrkB and α-adaptin was visualized by immunostaining with anti-TrkB (red) and anti-α-adaptin (green), respectively. B4 and B8 are magnified view of boxed region of B3 and B7, respectively.

(C) Schematic of TrkB immunostaining pattern in the inner EGL (EGLb) of sagittal sections of developing cerebellum. Cells marked "+" would be scored as correctly polarized. TrkB (red) and Zic (blue).

(D) Quantitative analysis of TrkB polarization toward IGL in EGLb in *bdnf* +/+ and −/− mice. Data shown represent the means ± SEM and were evaluated by two-tailed Student's t-test (*, $p < 0.001$; n=6).

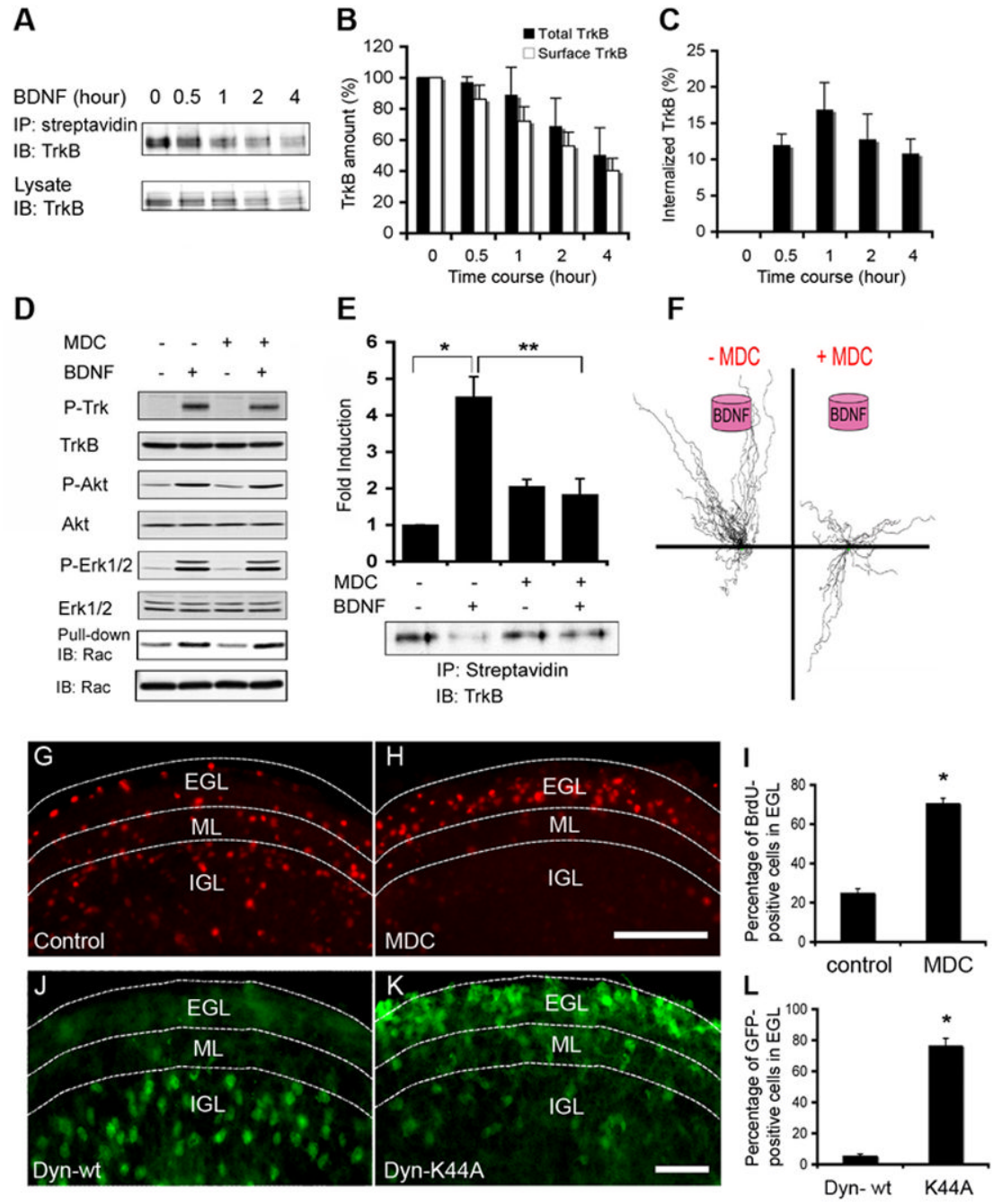

Figure 4. TrkB Receptor Endocytosis Is Required for BDNF-induced GCP Chemotaxis

(A) Time course of BDNF –induced TrkB endocytosis in GCPs. P6 GCPs were treated with BDNF for indicated time and cell surface molecules were labeled with NHS-SS-biotin. Cell lysates were precipitated with streptavidin sepharose. Surface TrkB receptors were visualized by Western blot analysis of the precipitated proteins with anti-TrkB. Total TrkB in lysates was visualized as a control (lower panel).

(B) Densitometry analysis of surface TrkB and total TrkB at various time course of BDNF treatment in 4A. Densitometry of TrkB bands was carried out as described in *Experimental Procedures*. Data shown represent means ± SEM (n=3).

(C) Calculation of internalized TrkB in 4A. Relative amount of internalized TrkBs were calculated by subtracting the percentage of surface TrkBs from the percentage of total TrkB at each time point. Data shown represent means ± SEM (n=3).
(D) The internalization inhibitor MDC does not block BDNF-triggered TrkB signaling. GCPs were pretreated with vehicle or MDC for 30 min, then stimulated with BDNF for 10 min. Cell lysates were subject to Western blot analysis with indicated antibodies.
(E) MDC inhibits BDNF-induced TrkB internalization and GCP chemotaxis. GCPs were pretreated with vehicle or MDC for 30 min and exposed to BDNF gradient. GCP migration was measured by real-time migration assay (top panel). Data were evaluated by z test (*, $p < 0.001$) and two-tailed Student's t-test (**, $p< 0.001$), respectively. MDC inhibition of BDNF-induced TrkB internalization in GCPs was assayed as described in 4A (lower panel).
(F) Superimposed path traces of migrating GCPs in experiments of 4E (n=3).
(G) – (I) MDC inhibits directed migration of GCPs from the EGL to the IGL in P7 organotypic slice cultures. (G) and (H), One representative picture derived from three independent experiments. *Scale bar*: 100μm. (I), Quantitative analysis of inhibitory effect of MDC treatment on GCP migration in organotypic slice cultures, data shown represent the means ± SEM from three independent experiments (*, $p < 0.001$ by two-tailed Student's t-test).
(J) – (L) Expression of dominant-negative dynamin K44A inhibits directed migration of GCPs from the EGL to the IGL in P7 cerebellar slice cultures. Wild-type (wt) dynamin (J) or dynamin K44A (K) expression is driven by the ubiquitin promoter followed by an IRES-eGFP expression cassette. GFP-positive cells (green) reflect the GCPs infected by virus. Representative picture derived from three independent experiments. *Scar bar*: 50 μm (J and K). (L), Quantitative analysis of Dyn-K44A effect on GCP migration in organotypic slice cultures, data shown represent the means ± SEM from three independent experiments (*, $p < 0.001$ by two-tailed Student's t-test).

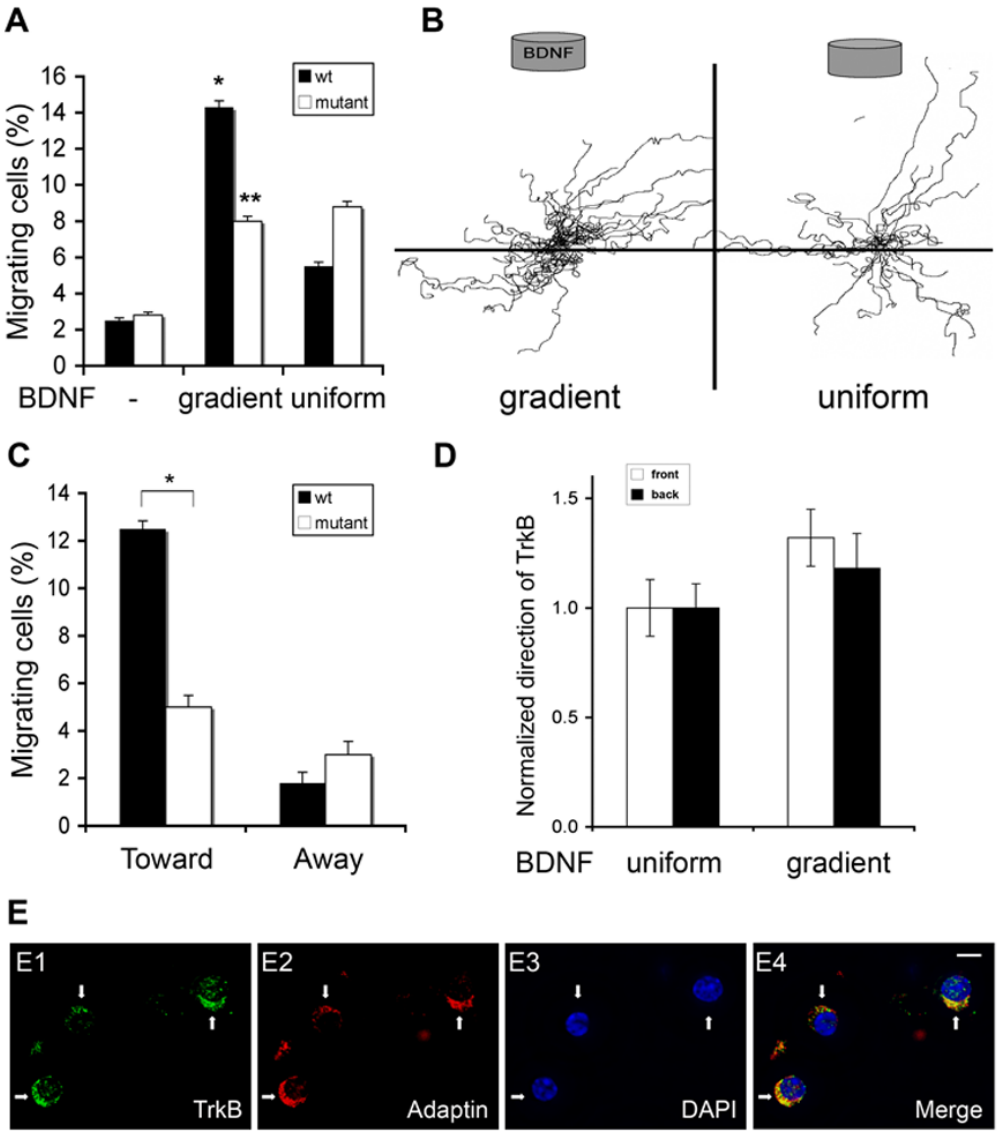

Figure 5. A BDNF Gradient Promotes Motility in GCPs from *bdnf* −/− Mice, but Does Not Lead to a Directional Response

(A) Quantitative analysis of the percentage of GCP migration of wild type and mutant mice from four independent experiments under three conditions (no BDNF, gradient and uniform BDNF, respectively). Data shown represent means ± SEM (n=4) and were evaluated by two-tailed Student's t test (*, differs from wild type migration both without BDNF and in uniform BDNF, $p < 0.001$; **, differ from *bdnf* −/− migration without BDNF, $p < 0.05$).

(B) The pathway traces of individual migrating GCPs of mutant mice from four independent experiments in 5A for two conditions (gradient BDNF and uniform BDNF, respectively) were superimposed on a common origin.

(C) Quantitative analysis of migration directionality of GCP migration from wild type and mutant mice when exposed to BDNF gradient from 5A. Data shown represent means ± SEM (n=4) and were evaluated by two-tailed Student's t-test. (*, $p < 0.005$).

(D) Quantitative analysis of TrkB localization at the front or the back of cell. GCPs were exposed to uniform or gradient BDNF for 12 hours, fixed and immunostained with anti-TrkB. TrkB localization was assessed by counting the percentage of cells with TrkB polarized toward

the agarose plug (front) or away (back). For each experiment, the percentage of cells with TrkB polarized to the front under uniform stimulation condition was set as 1. Data shown represent means ± SEM (n=4).

(E) A representative image of the experiments in 5D showing random localization of TrkB signaling endosomes in *bdnf* −/− GCPs in response to BDNF gradient. GCPs from P6 *bdnf* −/− mice were exposed to BDNF gradient for 12 hours, then fixed and stained with anti-α-adaptin (red) and anti-TrkB (green). DAPI staining visualizes nuclei (blue). Arrow indicates the GCPs with polarized TrkB signaling endosomes. BDNF source is on the top of images. *Scal bar*: 5 μm.

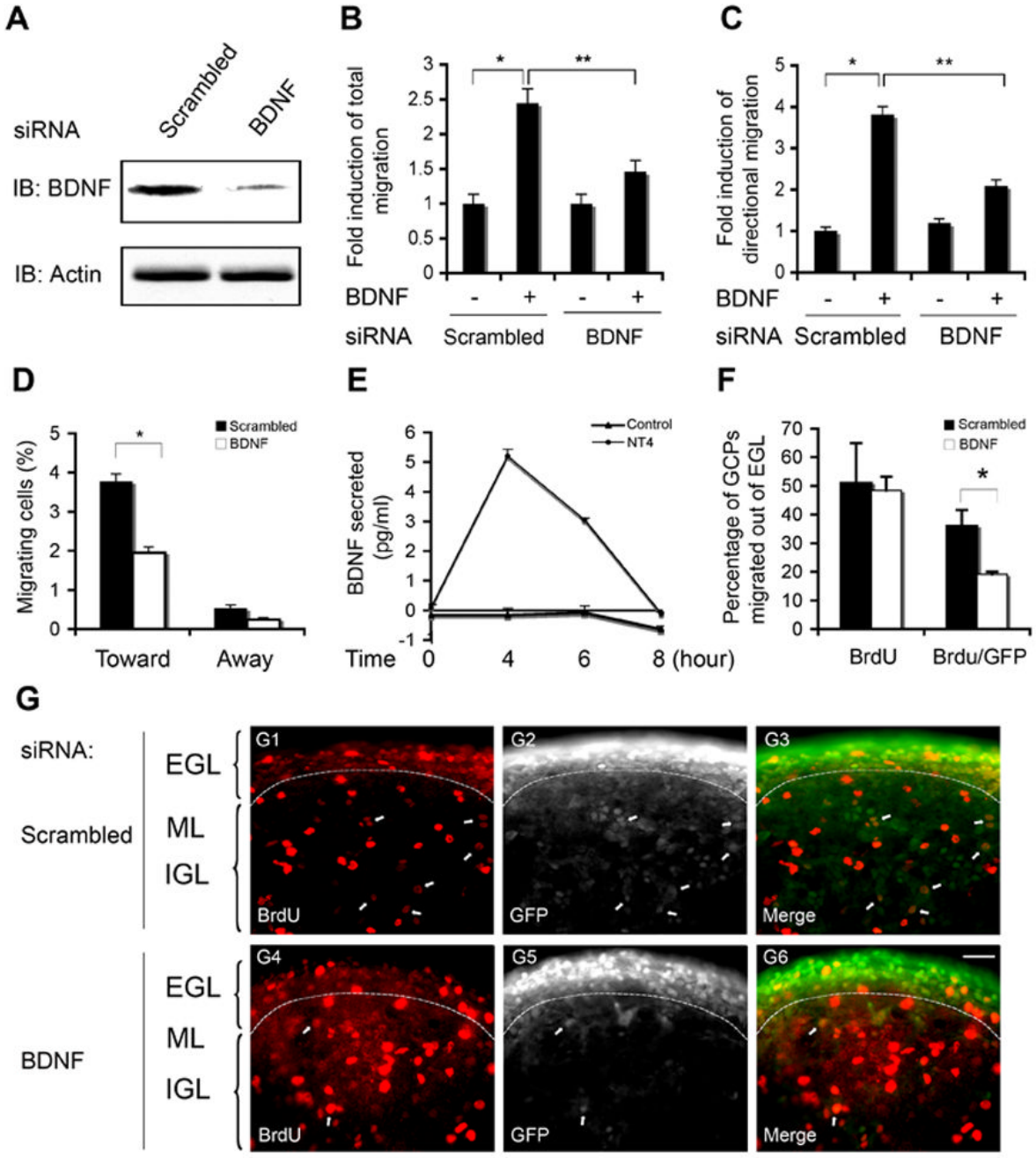

Figure 6. Autocrine BDNF Promotes GCP Chemotaxis

(A) Efficient blockade of BDNF expression by *bdnf* siRNA in GCPs. GCPs from P6 wild type mice were infected with lentivirus expressing *bdnf* siRNA or scrambled RNA and cultured for 48 hours. GCPs were lysed with RIPA buffer and cleared lysates were subject to Western blot analysis with anti-BDNF and anti-actin as a loading control.

(B) Acute knockdown of BDNF decreases GCP migration in an exogenous BDNF gradient. Wild type GCPs infected with *bdnf* siRNA or scrambled RNA lentivirus were subject to real-time migration assay in response to a BDNF gradient. Data shown represent mean ± SEM (n=3) and evaluated by z test (*, $p < 0.01$) and two-tailed Student's t-test (**, $p < 0.05$), respectively.

(C) Acute knockdown of BDNF impairs directional migration of GCPs. The directional migration of GCPs toward a BDNF gradient was analysed for experiments in 6B. Data were evaluated by z test (*, $p < 0.001$) and two-tailed Student's t-test (**, $p< 0.05$), respectively.
(D) Quantitative analysis of migration directionality of GCPs infected with BDNF siRNA lentivirus and control virus when exposed to BDNF gradient from 6B. Data shown represent means ± SEM (n=3) and were evaluated by two-tailed Student's t-test. (*, $p < 0.05$).
(E) NT4 stimulation of GCPs induces BDNF secretion. Dissociated GCPs were exposed to NT4 (50 ng/ml) or vehicle for indicated times, the media were collected, concentrated 10 fold and then analyzed for BDNF concentration released by GCPs by ELISA. Data shown represent means ± SEM (n=3).
(F) Acute knockdown of BDNF inhibits directional migration of GCPs in cerebellar slice cultures. Cerebellar slices (250 μm) were infected with lentivirus expressing *bdnf* siRNA or scrambled RNA for 24 hours, pulse-labeled with BrdU for 6 hours and then cultured for additional 36 hours before fixation. Slices were immunostained with anti-BrdU and anti-GFP. Data shown are from three independent experiments. The percentage of BrdU- or BrdU and GFP- positive cells in ML and IGL were determined. Data shown represent mean ± SEM (n=3) and were evaluated by two-tailed Student's t-test (*, $p < 0.001$).
(G) Representative images of the experiments in 6F. G1–G3, scrambled siRNA; G4–G6, *bdnf* siRNA. *Scale bar*: 25 μm. Arrow indicates BrdU (red) and GFP (white) double-positive GCPs.

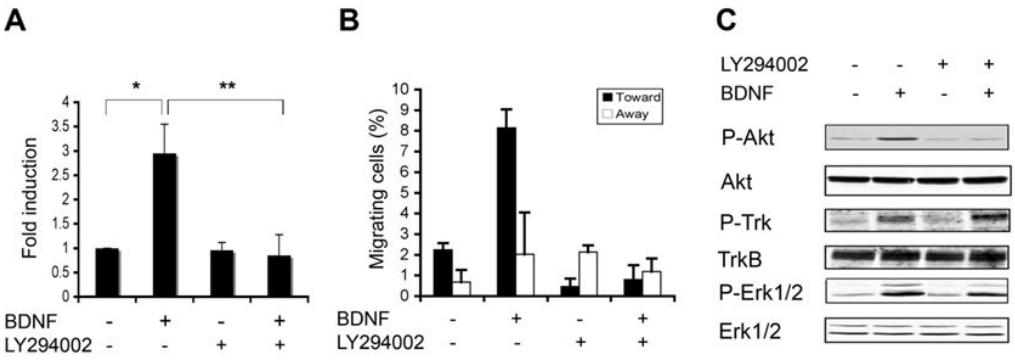

Figure 7. PI3 Kinase Pathway Is Essential for BDNF-induced GCP Chemotaxis

(A) PI3 kinase inhibitor LY294002 blocks BDNF-induced GCP migration. GCP real-time migration was analyzed from three independent experiments in the absence or presence of LY294002 (10 μM). Data were evaluated by z test (*, $p < 0.005$) and two-tailed Student's t-test (**, $p< 0.001$), respectively.

(B) The effect of LY294002 treatment on directionality of GCP migration in response to a BDNF gradient. LY294002 pre-treatment blocks directional migration of GCPs toward the BDNF source. Data shown represent quantitative analysis of the experiments in 7A.

(C) Western blot analyses show that LY294002 treatment efficiently inhibits BDNF-induced activation of PI3 kinase pathway while there is no effect on BDNF activation of TrkB and Erk in GCPs. Dissociated GCPs were pre-treated with vehicle or inhibitor for 30 min prior to BDNF addition.

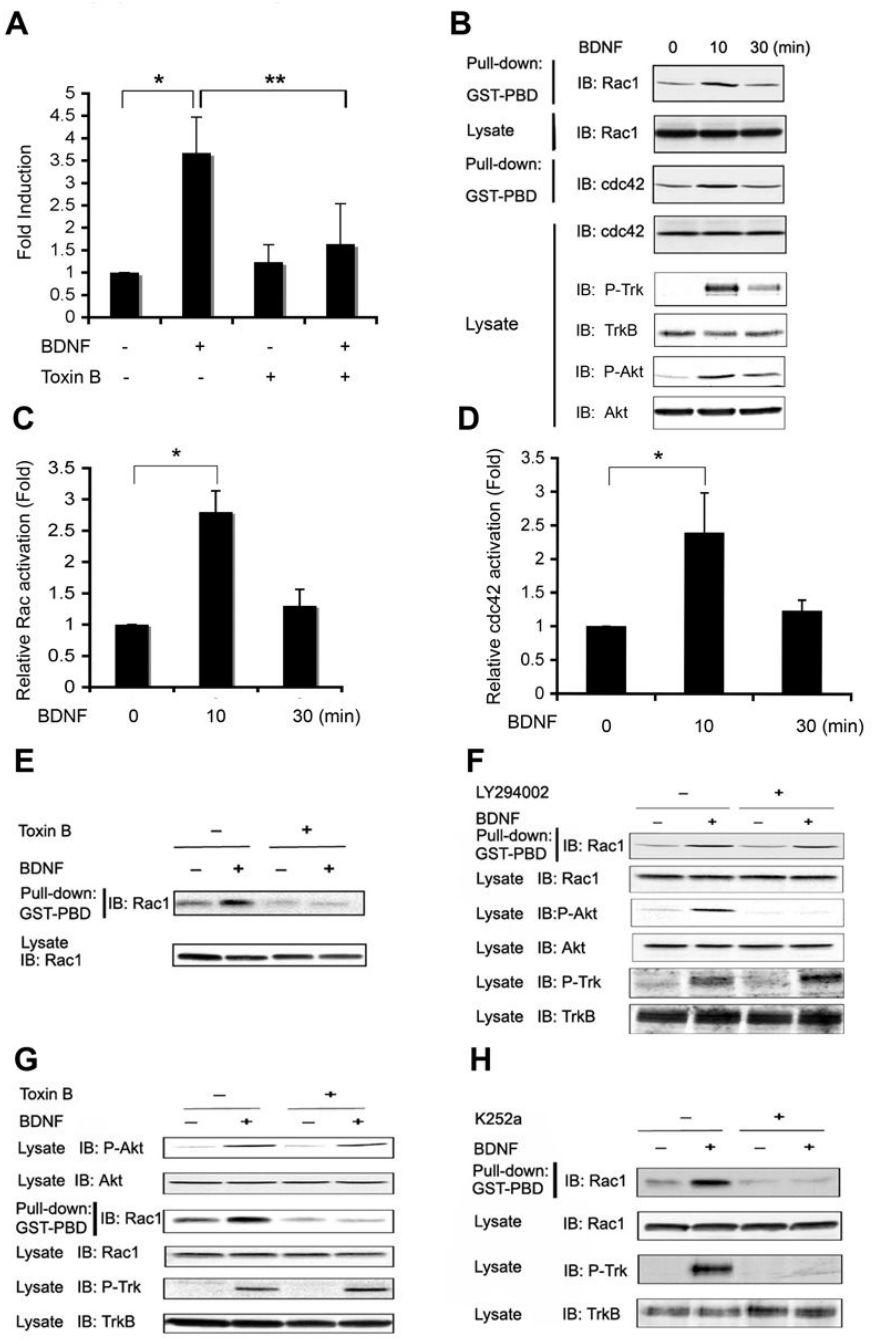

Figure 8. Activation of Rho Family GTPases Is Essential for BDNF-induced GCP Chemotaxis

(A) Real-time migration assays show that Toxin B, an inhibitor of Rho family GTPases, prevents BDNF-induced migration of GCPs. Data were evaluated by z test (*, $p < 0.005$) and two-tailed Student's t-test (**, $p < 0.001$), respectively.

(B) Time course of Rac and cdc42 activation in response to BDNF by Western blot analysis. Dissociated GCPs were treated with BDNF for the indicated time, and activation of Rac and cdc42 was measured using GST-PBD to pull down activated proteins that are visualized by Western blot analysis with anti-Rac or anti-cdc42 antibody. Activation of TrkB and Akt as well as total levels of each protein in cell lysates are shown.

(C) Quantitative analysis of Rac activation induced by BDNF in 8B was carried out by densitometry as described in *Experimental Procedures*. Data shown represent means ± SEM (n=3) and were evaluated by z test (*, $p< 0.001$).
(D) Quantitative analysis of cdc42 activation induced by BDNF in 8B was carried out by densitometry as described in *Experimental Procedures*. Data shown represent means ± SEM (n=3) and were evaluated by z test (*, $p< 0.05$).
(E) Rho family GTPases inhibitor Toxin B abolishes BDNF-induced Rac activation. Dissociated GCPs were pre-treated with Toxin B for 30 min prior to BDNF treatment. GTP-bound, active Rac and total Rac were measured by pull-down assay.
(F) PI3 kinase pathway inhibitor does not block BDNF-induced Rac activation. Dissociated GCPs were pre-treated with PI3 kinase inhibitor LY294002 (10 μM) for 30 min and then treated with BDNF for 10 min. Rac activation was measured as described above. Activation of Akt and TrkB were assessed with phospho-specific antibodies.
(G) Inhibition of Rac activation fails to abrogate BDNF-induced activation of PI3 kinase pathway. GCPs were pretreated with 40 ng/ml Toxin B for 30 min prior to BDNF addition.
(H) TrkB kinase activity is needed for BDNF-induced Rac activation in GCPs. Dissociated GCPs were pretreated with 200 nM K252a for 30 min and then stimulated with BDNF for 10 min. Total levels of each protein are also shown.

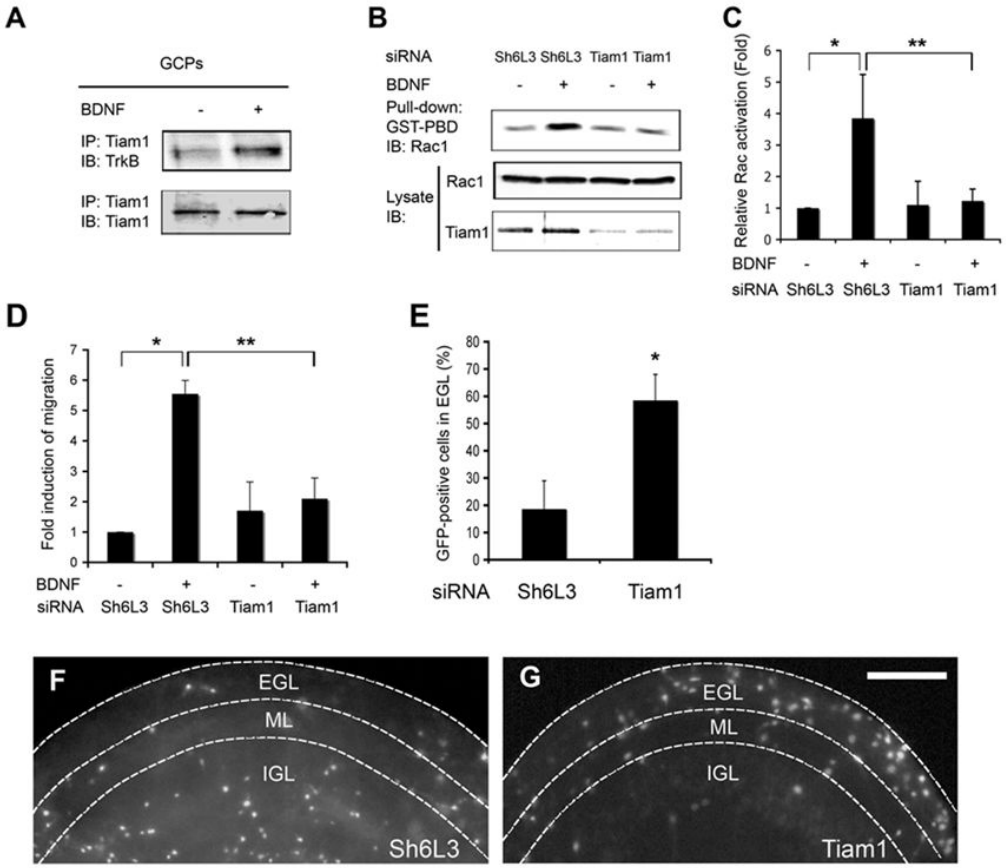

Figure 9. Tiam1 Interacts with TrkB, and Mediates BDNF-induced Rac Activation and Chemotaxis

(A) Tiam1 interacts with TrkB in GCPs. Dissociated GCPs were stimulated with or without BDNF for 10 min and cell lysates were immunoprecipitated with anti-Tiam1 followed by Western blot analysis with anti-TrkB. Membrane was stripped and reprobed with anti-Tiam1.

(B) Tiam1 mediates BDNF-induced Rac activation. GCPs were infected with Tiam1 siRNA lentivirus or control lentivirus expressing luciferase siRNA (Sh6L3). After 48 hours of infection, GCPs were treated with or without 50 ng/ml BDNF for 10 min. Rac activation was measured by GST-PBD pull-down assay. Total levels of Rac and Tiam1 in the lysates are also shown.

(C) Relative Rac activation was quantitatively analyzed by densitometry of three independent experiments. Data were evaluated by z test (*, $p < 0.001$) and two-tailed Student's t-test (**, $p < 0.005$), respectively.

(D) Attenuated expression of Tiam1 inhibits BDNF-induced migration of GCPs. Dissociated GCPs were infected with Tiam1 siRNA lentivirus or control lentivirus expressing luciferase siRNA. After 48 hours of infection, BDNF-induced migration of virus-infected GCPs was measured by real-time migration assay. Data were evaluated by z test (*, $p < 0.001$) and two-tailed Student's t-test (**, $p < 0.005$), respectively.

(E) Attenuated expression of Tiam1 blocks GCP directed migration from EGL to IGL in organotypic slices. Data shown represent means ± SEM (n=3) and were evaluated by two-tailed Student's t-test (*, $p < 0.001$).

(F) and (G) Representative pictures from the experiments in 9E.

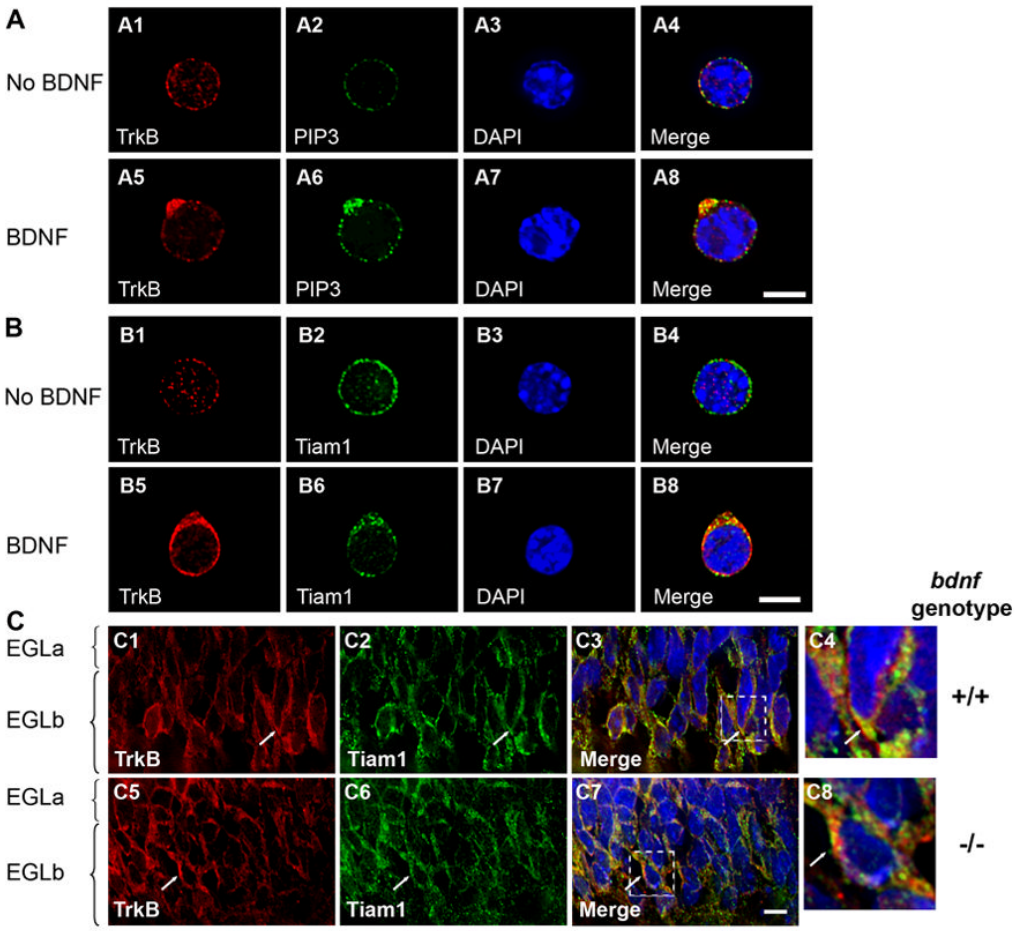

Figure 10. BDNF-dependent Polarization of Signaling Molecules at the Leading Edge of GCPs *in vitro* and *in vivo*

GCPs were or were not exposed to uniform or gradient BDNF for 12 hours, fixed and immunostained as indicated. The BDNF source is at the top (panel A and B). Cerebellar sections from P6 *bdnf* +/+ or −/− mice were used for immunostaining as indicated (panel C). DAPI staining visualizes nuclei (blue). Scale bars: 5 μm.

(A) TrkB receptors colocalize with PI (3,4,5) P3 phospholipids at the leading edge of GCPs as shown by immunofluorescent staining with anti-TrkB (red) and anti-PI (3,4,5) P3 phospholipids (green).

(B) TrkB receptors colocalize with Tiam1 at the leading edge of GCPs as shown by immunofluorescent staining with anti-TrkB (red) and anti-Tiam1 (green).

(C) Polarized TrkB(s) colocalize with Tiam1 within punctate structures at the leading edge of migrating GCPs from *bdnf* +/+ mice (C1–C4) at the deeper EGL (EGLb), whereas these molecules are distributed randomly in GCPs from *bdnf* −/− animals (C5–C8). The colocalization of TrkB and Tiam1 within GCPs was visualized by immunostaining with anti-TrkB (red) and anti-Tiam1 (green). C4 and C8 are magnified view of boxed region of C3 and C7, respectively.